

Measuring age, metallicity and abundance ratios from absorption line indices

Rosaria Tantalo & Cesare Chiosi

Department of Astronomy, University of Padova, Vicolo dell'Osservatorio 2, 35122 Padova, Italy
E-mail: tantalo@pd.astro.it; chiosi@pd.astro.it

Submitted: November 2003; Revised: May 2004

ABSTRACT

In this study we present detailed calculations of absorption line indices on the Lick System based on the new stellar models by Salasnich et al. (2000) incorporating the enhancement of α -elements both in the opacity and in the chemical abundances. The models span large ranges of initial masses, chemical compositions, and ages, and are calculated for both solar and enhanced abundance ratios $[X_{\text{el}}/\text{Fe}]$ of α -elements. With these models and the so-called *Response Functions* of Tripicco & Bell (1995), we calculate the indices for Single Stellar Populations (SSPs) of different age, metallicity and degree of enhancement. Starting from the widely accepted conviction that H_{β} is a good age indicator, that $[\text{MgFe}]$ is most sensitive to metallicity, and indices like Mg_b , Mg_2 and others are most sensitive to metallicity and degree of enhancement, we made use of the triplet H_{β} , Mg_b and $\langle\text{Fe}\rangle$, and *Minimum-Distance Method* proposed by Trager et al. (2000b) to estimate the age, metallicity and enhancement degree for the galaxies of the González (1993) sample, and compare the results with those by Trager et al. (2000b) and Thomas et al. (2003a). Since very large differences are found, in particular as far as the age is concerned, ours are systematically older than those of Trager et al. (2000b) and Thomas et al. (2003a), we analyze in a great detail all possible sources of disagreement, going from the stellar models and SSPs to many technical details of the procedure to calculate the indices, and finally the pattern of chemical elements (especially when α -enhanced mixtures are adopted). Each of the above aspects of the problem bears on the final result: amazingly enough, at increasing complexity of the underlying stellar models and SSPs, the uncertainty increases. However, the key issue of the analysis is that at given metallicity Z and enhancement factor, the specific abundance ratios $[X_{\text{el}}/\text{Fe}]$ adopted for some elements (e.g. O, Mg, Ti, and likely others) dominate the scene because with the Tripicco & Bell (1995) *Response Functions* they may strongly affect indices like H_{β} and the age in turn. In brief, with the ratio $[\text{Ti}/\text{Fe}]=0.63$ adopted by Salasnich et al. (2000), H_{β} at old ages turned out to be larger than the mean observational value, and therefore the age was forced to very old values in order to recover the observations. In contrast, the results by Trager et al. (2000b) and Thomas et al. (2003a) are immediately recovered if their $[\text{Ti}/\text{Fe}]$ ratios are adopted, i.e. $[\text{Ti}/\text{Fe}]=0.0$ or 0.3 , respectively. We have also analyzed how the galaxy ages, metallicities and degrees of enhancement vary with the triplets of indices in usage. To this aim we turn to the Trager “*IDS Pristine*” sample which contains many more galaxies and a much wider list of indices than the González sample. The solution is not unique in that reflecting the poor ability of most indices to disentangle among the three parameters. Finally, at the light of the above results and points of uncertainty, we have drawn some remarks on the interpretation of the distribution of early-type galaxies in popular two-indices planes, like H_{β} vs. $[\text{MgFe}]$. We argue that part of the scatter along the H_{β} axis observed in this plane could be attributed instead of the age, the current explanation, to a spread both in the degree of enhancement and some abundance ratios. If so, another dimension is added to the problem, i.e. the history of star formation and chemical enrichment in individual galaxies. The main conclusion of this study is that deriving ages, metallicities and degree of enhancement from line indices is a cumbersome affair whose results are still uncertain.

Key words: Galaxies: elliptical – Galaxies: chemical evolution – Galaxies: metallicities – Galaxies: ages – Galaxies: photometry

arXiv:astro-ph/0305247v3 16 Jun 2004

1 INTRODUCTION

Over the years, much effort has been spent to infer from observational data the age, metallicity, and enhancement of the α -elements of the stellar content in early-type galaxies (EGs) (Bressan et al. 1996; Tantalo 1998; Tantalo et al. 1998; Jørgensen 1999; Trager et al. 2000b,a; Kuntschner 2000; Kuntschner et al. 2001; Vazdekis et al. 2001; Davies et al. 2001; Maraston et al. 2003; Thomas et al. 2003a,b; Thomas & Maraston 2003).

Determining the age and metallicity is a cumbersome affair hampered by the fact that the spectral energy distribution of an old metal-poor stellar population may happen to be the same of a young metal-rich one. This is otherwise known as the *age-metallicity degeneracy* pointed out long ago by Renzini & Buzzoni (1986).

A promising way-out is perhaps offered by the absorption line indices defined by the Lick group (Worthey 1992; Worthey et al. 1994), which seem to have the potential of partially resolving the *age-metallicity degeneracy*. An extensive use of the two indices diagnostics is currently made in order to infer the age and the metallicity of early-type galaxies (Kuntschner & Davies 1998; Jørgensen 1999; Kuntschner 1998, 2000; Kuntschner et al. 2001; Trager et al. 2000b; Vazdekis et al. 2001; Davies et al. 2001; Poggianti et al. 2001; Maraston et al. 2003; Thomas et al. 2003a,b; Thomas & Maraston 2003).

The problem is, however, further complicated by a third parameter, i.e. the abundance ratio $[\alpha/\text{Fe}]$ (where α stands for all chemical elements produced by α -captures on lighter nuclei). Absorption line indices like Mg_2 and $\langle\text{Fe}\rangle$ measured in the central regions of galaxies are known to vary passing from one galaxy to another (González 1993; Trager et al. 2000b,a). Looking at the correlation between Mg_2 and $\langle\text{Fe}\rangle$ (or similar indices) for the galaxies in the above quoted samples, Mg_2 increases faster than $\langle\text{Fe}\rangle$, which is interpreted as due to enhancement of α -elements in some galaxies. In addition to this, since the classical paper by Burstein et al. (1988), the index Mg_2 is known to increase with the velocity dispersion (and hence mass and luminosity) of the galaxy. Standing on this body of data the conviction arose that the degree of enhancement in α -elements ought to increase passing from dwarf to massive EGs (Faber et al. 1992; Worthey et al. 1994; Matteucci 1994, 1997; Matteucci et al. 1998). The simplest and most widely accepted interpretation is the one based on the different duration of the star forming period and the different contribution to α -elements and Fe by Type II supernovae from massive stars (mostly producing α -elements) and Type Ia supernovae from accreting white dwarfs in binary systems (mostly generating Fe). Since the minimum mean time scale for a binary mass-accreting white dwarf to get the supernova stage is ≥ 0.5 Gyr, the iron contamination by Type Ia supernovae occurs later as compared to the ones of Type II (Greggio & Renzini 1983). With the standard supernova driven galactic wind model (SDGW) by Larson (1974) and classical initial mass function, to reproduce the observed trend of the $[\alpha/\text{Fe}]$ -mass relationship, the total duration of the star forming activity ought to decrease at increasing galaxy mass. Long ago Larson (1974) suggested that the Color-Magnitude Relation stems from a mass-mean metallicity relation, whereby the massive EGs are more metal-rich. He also proposed the SDGW mecha-

nism as the key process by which massive EGs, owing to their deeper gravitational potential, retain gas and form stars for longer periods of time than the low-mass ones. *This is the opposite of what implied by the trend in α -elements.* The kind of behavior for the star formation history in EGs required by the α -enhancement has been suggested by Bressan et al. (1996) and Tantalo et al. (1998) on the base of their properties in the two indices planes, and more recently confirmed by Poggianti et al. (2001) and the N-body-Tree-SPH models of EGs by Chiosi & Carraro (2002).

In presence of α -enhanced chemical compositions, ages and metallicities of EGs should be derived from indices in which this effect is taken into account. As long ago noticed by Worthey et al. (1992) and Weiss et al. (1995), indices for α -enhanced chemical mixtures of given total metallicity are expected to differ from those of the standard case.

The first attempt to simultaneously derive ages, metallicities and $[\alpha/\text{Fe}]$ ratios for the early-type galaxies of the González (1993) sample is by Tantalo et al. (1998) by means of the so-called Δ -Method in which the effect of different ratios $[\alpha/\text{Fe}]$ on theoretical indices has been included assuming the Borges et al. (1995) calibration for Mg_2 and a suitable relationship between total metallicity Z and iron content $[\text{Fe}/\text{H}]$ (Bressan et al. 1996; Tantalo et al. 1998). Similar attempt was made by Trager et al. (2000b, TFWG00) using different calibrations (Tripicco & Bell 1995) but reaching similar results.

However, the SSPs adopted by Bressan et al. (1996), Tantalo (1998), Tantalo et al. (1998) and also Tantalo et al. (1998) were actually calculated from the Padova library of stellar models with solar partition of elements and old opacities (Bertelli et al. 1994). The SSPs adopted by TFWG00 are taken from the even older SSPs library by Worthey (1994). Recently Thomas et al. (2003a), Thomas et al. (2003b, TMB03), Maraston et al. (2003) and Thomas & Maraston (2003) presented synthetic absorption line indices on the Lick system for SSPs with variable chemical abundances calibrated on a sample of Milky Way Globular Clusters whose metallicities vary from $Z_{\odot}/30$ to Z_{\odot} . In general almost all of the above studies are based on stellar models whose chemical composition (in particular the abundance ratios) are not the same as those used to derive the indices. Stellar models and indices are in a sense decoupled. Since in the meantime more recent stellar models, isochrones, and SSPs with updated physical input and α -enhanced chemical mixtures have become available (Salasnich et al. 2000, SGWC00), in the present study we intend to bridge the gap and to generate and use indices that are fully compatible with the stellar models underneath, and cast light on how much the results would depend on the internal consistency for the chemical parameters.

The plan of the paper is as follows. Section 2 defines the so-called *enhancement factor* for a mixture in which the abundance of α -elements with respect to that of Fe is enhanced as compared to the Solar Mix. Section 3 presents a brief description of the new stellar models and SSPs by SGWC00 in which α -enhanced chemical abundances are adopted. Section 4 shortly introduces the definition of the absorption line indices for a single star, and their corresponding integrated values for SSPs. Section 5 presents three different ways or “calibrations” to include the effect of α -enhanced chemical compositions on absorption line in-

dices and the choice we have made. Section 6 describes the formalism we have used to derive the integrated indices for SSPs. Section 7 firstly presents the indices for SSPs of different age, metallicity and enhancement factor, secondly illustrates the method to derive these parameters from the observational indices, contains some preliminary results for a selected sample of EGs, and finally compares them with those from previous studies. Since very large differences are found, in Section 8 we analyze in detail the many reasons why such large differences may occur, i.e. the stellar models in use, the coverage of evolutionary phases, and other technical aspects in the calculations of SSP indices. Section 9 is dedicated to the specific subject of the effects caused by using different pattern of abundances for α -enhanced elements, pointing out that this is the parameter driving the whole subject. Specifically we investigate the role played by some important elements, and argue that the source of the disagreement between the results obtained by TFWG00, Thomas et al. (2003a) and the ones presented here is entirely due to the different abundance ratio [Ti/Fe] adopted by SGWC00 (Section 9.6). In Section 10 we examine whether the solution for the age, metallicity and enhancement factor is unique, in the sense that the same result is obtained using different combinations of indices in groups of three. As expected no unique answer is found. To overcome the difficulty we check whether imposing the simultaneous fit of many indices the solution can be better constrained, In Section 11 we draw some remarks on the widely adopted two-indices plane diagnostics to estimate the age, metallicity, and degree of enhancement of α -elements. Finally, a summary of the results of this study and some concluding remarks are presented in Section 12.

2 CHEMICAL ENHANCEMENT: DEFINITION

In presence of enhancement in α -elements one has to modify the relationship between the total metallicity Z and the iron content [Fe/H]. This is made by suitably defining the enhancement parameter Γ . Following Tantaló et al. (1998), let us split the metallicity Z in the sum of two terms

$$Z = \sum_j X_j + X_{\text{Fe}} \quad (1)$$

where X_j are the abundances by mass of all heavy elements but Fe, and X_{Fe} is the same for Fe. Recasting eqn. (1) as

$$Z = \frac{X_{\text{Fe}}}{X_{\text{H}}} X_{\text{H}} \left[1 + \frac{\sum_j X_j}{X_{\text{Fe}}} \right] \quad (2)$$

and normalizing it to the solar values we get

$$\left(\frac{Z}{Z_{\odot}} \right) = \left(\frac{X_{\text{Fe}}}{X_{\text{H}}} \right) \left(\frac{X_{\text{H}}}{X_{\text{Fe}}} \right)_{\odot} \left(\frac{X_{\text{H}}}{X_{\text{H},\odot}} \right) \frac{\left[1 + \frac{\sum_j X_j}{X_{\text{Fe}}} \right]}{\left[1 + \frac{\sum_j X_j}{X_{\text{Fe}}} \right]_{\odot}} \quad (3)$$

from which we finally obtain

$$[\text{Fe}/\text{H}] = \log(Z/Z_{\odot}) - \log(X/X_{\odot}) - \Gamma \quad (4)$$

For solar metallicity Z_{\odot} and solar-scaled mixture ($\Gamma=0$),

eqn. (4) yields [Fe/H]=0. The definition of Γ is obvious. There in after Γ is referred to as the *total enhancement parameter*. This relation is useful to re-scale the Fe content in presence of $\Gamma \neq 0$ and vice-versa.

To avoid misunderstanding it may be useful to briefly describe the practical derivation of Γ for a set of elements, whose total metal abundance is Z , but in which a sub-group have abundances enhanced with respect of the corresponding solar value. Let denote with N_j the number density of the generic element j with mass abundance X_j and define the quantity A_j as in Grevesse et al. (1996)

$$A_j = \log \left(\frac{N_j}{N_{\text{H}}} \right) + 12 \quad (5)$$

The abundance by mass with respect to iron is given by

$$\left[\frac{X_j}{X_{\text{Fe}}} \right] = \log \left(\frac{X_j}{X_{\text{Fe}}} \right) - \log \left(\frac{X_j}{X_{\text{Fe}}} \right)_{\odot} \quad (6)$$

which corresponds to

$$\left[\frac{X_j}{X_{\text{Fe}}} \right] = \left[\frac{X_j}{X_{\text{H}}} \right] - \left[\frac{X_{\text{Fe}}}{X_{\text{H}}} \right] \quad (7)$$

This can be rewritten as function of the number density N_j in the following way

$$\left[\frac{X_j}{X_{\text{Fe}}} \right] = \left[\frac{N_j}{N_{\text{H}}} \right] - \left[\frac{N_{\text{Fe}}}{N_{\text{H}}} \right] \quad (8)$$

or in terms of A_j

$$\left[\frac{X_j}{X_{\text{Fe}}} \right] = (A_j^{\text{enh}} - A_j^{\odot}) - (A_{\text{Fe}}^{\text{enh}} - A_{\text{Fe}}^{\odot}) \quad (9)$$

Keeping constant the number density of iron, i.e. $(A_{\text{Fe}}^{\text{enh}} - A_{\text{Fe}}^{\odot})=0$, we get

$$A_j^{\text{enh}} = \left[\frac{X_j}{X_{\text{Fe}}} \right] + A_j^{\odot} \quad (10)$$

Using $[X_j/X_{\text{Fe}}]$ and A_j^{\odot} taken from observational data and Grevesse et al. (1996), respectively, we can calculate the new mass abundances for the solar-scaled case by means of eqn. (5). In general, the summation of the new mass abundances in the set of enhanced elements will be different from the assigned total metallicity. The mass abundances must be rescaled to the true value X'_j by means of the relation

$$X'_j = \frac{X_j}{\sum X_j} \quad (11)$$

Finally the total enhancement factor Γ is simply given by

$$\Gamma = -\log \left(\frac{X'_{\text{Fe}}}{X_{\text{Fe}}^{\odot}} \right) \quad (12)$$

which is another way of defining the enhancement factor fully equivalent to that of eqn. (4).

A slightly different definition of enhancement has been adopted by TFWG00 and TMB03 which however are fully equivalent to ours so that straight comparison is possible.

Table 1. The [Fe/H] ratio for solar-scaled and α -enhanced mixtures as a function of the initial chemical composition [X,Y,Z].

			$\Gamma = 0$	$\Gamma = 0.35$	$\Gamma = 0.50$
Z	Y	X	[Fe/H]	[Fe/H]	[Fe/H]
0.008	0.248	0.7440	-0.3972	-0.7529	-0.8972
0.019	0.273	0.7080	0.0000	-0.3557	-0.5000
0.040	0.320	0.6400	0.3672	0.0115	-0.1328
0.070	0.338	0.5430	0.6824	0.3267	0.1715

Finally, it is worth calling attention that at given total metallicity Z different patterns of $[X_j/X_{Fe}]$ may yield the same total enhancement factor Γ . This fact bears very much on the correction of indices for enhancement because each elemental species brings a different effect (see Section 5.2 below).

3 STELLAR MODELS WITH α -ENHANCED CHEMICAL COMPOSITIONS

SGWC00 have presented four sets of stellar models with different initial chemical compositions [$Y=0.250$, $Z=0.008$], [$Y=0.273$, $Z=0.019$], [$Y=0.320$, $Z=0.040$] and [$Y=0.390$, $Z=0.070$], initial masses from 0.15 to 20 M_{\odot} , helium-to-metal enrichment law $Y = Y_p + 2.25Z$ ($Y_p=0.23$ is the primordial helium abundance), and both solar and α -enhanced partitions of chemical elements.

In Table 1 we list the usual parameters X , Y and Z defining the initial chemical composition of a star and the corresponding [Fe/H] ratio for solar-scaled and α -enhanced mixtures. Columns (1) through (3) give the initial chemical composition of the adopted stellar models, whereas columns (4), (5) and (6) list the values of [Fe/H] for the standard solar-scaled composition ($\Gamma=0$), the α -enhanced mixture ($\Gamma=0.35$) adopted by SGWC00¹, and another choice for an α -enhanced composition ($\Gamma=0.50$) calculated by us for the purposes of this study and to be discussed below.

Table 2 lists the detailed pattern of elements and abundance ratios adopted by SGWC00 for the solar-scaled compositions ($\Gamma=0$), the α -enhanced mixtures with $\Gamma=0.35$, and our case with $\Gamma=0.50$. Columns (2), (4) and (8) show the abundance A_{el} of elements in logarithmic scale, columns (3), (5) and (9) display the ratio X_{el}/Z , columns (6) and (10) list the ratio $[X_{el}/Fe]$, and finally columns (7) and (11) show the ratio $[X_{el}/H]$.

The enhancement factors for individual species come from the determinations of chemical abundances in metal-poor field stars by Ryan et al. (1991). We call attention on the high enhancement factor for Ti, which amounts to $[Ti/Fe]=0.63$. The analysis below will clarify that the abundance of Ti bears very much on the final result, in particular as far as the H_{β} is concerned. More recent determinations by

Carney (1996) and Habgood (2001) of the $[Ti/Fe]$ in globular clusters yield $\langle[Ti/Fe]\rangle \simeq 0.25-0.30$. A similar study by Gratton et al. (2003) of abundances for a sample of metal-poor stars (150 objects in total) with accurate parallaxes yields $\langle[Ti/Fe]\rangle \simeq 0.20 \pm 0.05$ with long tails on both sides, the highest values however rarely exceeding 0.4. In spite of this, since the SGWC00 models have been calculated with $[Ti/Fe]=0.63$, we adopt this value throughout our study to compare the indices and their follow up with those of similar studies. Only at very end we will discuss the consequences of choosing different (lower) enhancement factors for this element.

The stellar models calculated by SGWC00 for $\Gamma=0$ and $\Gamma=0.35$ extend from the ZAMS up to either the start of the thermally pulsing asymptotic giant branch (TP-AGB) phase or carbon ignition. The major novelty of these stellar models with respect to previous calculations (e.g Bertelli et al. 1994; Girardi et al. 1996) is the opacity whose chemical mixture is the same of the stellar models. No details on the stellar models are given here; they can be found in SGWC00. Suffice it to mention that: (i) in low mass stars passing from the tip of red giant branch (T-RGB) to the HB or clump, mass-loss by stellar winds is included according to the Reimers (1975) rate with $\eta=0.45$; (ii) the whole TP-AGB phase is included in the isochrones with ages older than 0.1 Gyr according to the algorithm of Girardi & Bertelli (1998) and Girardi et al. (2000). Because of the opacities used by SGWC00 the new tracks of high metallicity ($Z=0.070$) do not develop the so-called hot horizontal branch (H-HB) and AGB-manqu  phase for low mass stars (see Greggio & Renzini 1990; Bressan et al. 1994, for all details) thus affecting a potential source of energy in the UV and visible ranges of the spectra with some important consequences for indices like H_{β} , $H_{\gamma F}$, etc. Finally for the four sets of stellar models the corresponding isochrones and SSPs are calculated².

4 ABSORPTION LINE INDICES FOR SSPS

Although the definition of the absorption line indices and how these are calculated for SSPs can be found in the original papers by Burstein et al. (1984), Faber et al. (1985), Worthey (1992), Worthey et al. (1994), and Bressan et al. (1996), it may be useful to summarize here the various steps of the procedure. For the sake of easy comparison, we strictly follow the notation adopted by Maraston et al. (2003).

The definition of an absorption line index with pass-band Δ_{λ} is different according to whether it is measured in equivalent width (EW) or magnitude as given by

$$\begin{aligned}
 I_1 &= \Delta_{\lambda} \left(1 - \frac{F_1}{F_c} \right) && \text{in EW} \\
 I_1 &= -2.5 \log \left(\frac{F_1}{F_c} \right) && \text{in Mag}
 \end{aligned}
 \tag{13}$$

where F_1 and F_c are the fluxes in the line and pseudo-continuum, respectively. Since the Lick system of indices (Burstein et al. 1984; Faber et al. 1985; Worthey et al. 1994)

¹ It is worth noticing that SGWC00 have enhanced the α -elements (see their Table 1 and Table 2 in this work) in such a way that the iron abundances for solar metallicity is equal to $[Fe/H]=-0.3557$ or equivalently $\Gamma \simeq 0.35$

² The complete grids of stellar tracks, isochrones and SSPs are available on the web site <http://pleiadi.pd.astro.it>.

Table 2. Abundance ratios for the solar-scaled and α -enhanced mixtures adopted in this study. The case for $\Gamma = 0.35$ is the same as in SGWC00, the case of $\Gamma = 0.50$ has been extrapolated by us (see the text for details).

Element	$\Gamma = 0$		$\Gamma = 0.35$				$\Gamma = 0.50$			
	A_{el}	X_{el}/Z	A_{el}	X_{el}/Z	$[X_{\text{el}}/\text{Fe}]$	$[X_{\text{el}}/\text{H}]$	A_{el}	X_{el}/Z	$[X_{\text{el}}/\text{Fe}]$	$[X_{\text{el}}/\text{H}]$
O	8.870	0.482273	9.370	0.672836	0.50	+0.1442	9.570	0.770549	0.70	+0.2035
Ne	8.080	0.098668	8.370	0.084869	0.29	-0.0658	8.490	0.079983	0.41	-0.0912
Mg	7.580	0.037573	7.980	0.041639	0.40	+0.0441	8.140	0.043451	0.56	+0.0631
Si	7.550	0.040520	7.850	0.035669	0.30	-0.0558	7.970	0.033806	0.42	-0.0787
S	7.210	0.021142	7.540	0.019942	0.33	-0.0258	7.670	0.019498	0.46	-0.0352
Ca	6.360	0.003734	6.860	0.005209	0.50	+0.1441	7.060	0.005970	0.70	+0.2038
Ti	5.020	0.000211	5.650	0.000387	0.63	+0.2634	5.890	0.000495	0.87	+0.3703
Ni	6.250	0.004459	6.270	0.002056	0.02	-0.3371	6.280	0.001503	0.03	-0.4723
C	8.550	0.173285	8.550	0.076451	0.00	-0.3553	8.550	0.054828	0.00	-0.4998
N	7.970	0.053152	7.970	0.023450	0.00	-0.3553	7.970	0.016827	0.00	-0.4995
Na	6.330	0.001999	6.330	0.000882	0.00	-0.3553	6.330	0.000632	0.00	-0.5001
Cr	5.670	0.001005	5.670	0.000443	0.00	-0.3557	5.670	0.000318	0.00	-0.4997
Fe	7.500	0.071794	7.500	0.031675	0.00	-0.3557	7.500	0.022751	0.00	-0.4991

stands on a spectra library with fixed mean resolution of 8 \AA , whereas most of the spectral libraries in use have a different resolution, the straightforward application of eqns. (13) is not possible. The difficulty is with F_1 which depends on the spectral resolution. To overcome this problem, the so-called *Fitting Functions* have been introduced. They express the indices measured on the observed spectra of a large number of stars with known gravity, T_{eff} , and chemical composition as functions of these parameters (Worthey et al. 1994).

Given these premises, the integrated indices of SSPs can be derived in the following way. We start from the flux in the absorption line of the generic i -th star of the SSP, $F_{1,i}^*$

$$F_{1,i}^* = F_{c,i}^* \left(1 - \frac{I_{1,i}^*}{\Delta_\lambda} \right) \quad \text{in EW} \quad (14)$$

$$F_{1,i}^* = F_{c,i}^* 10^{-0.4I_{1,i}^*} \quad \text{in Mag}$$

where $I_{1,i}^*$ is the index of the i -th star computed inserting in the *Fitting Functions* the values of T_{eff} , gravity, and chemical composition of the star, $F_{c,i}^*$ is the pseudo-continuum flux, and $F_{1,i}^*$ is the flux in the passband. The flux $F_{c,i}^*$ is calculated by interpolating to the central wavelength of the absorption line, the fluxes in the midpoints of the red and blue pseudo-continuum bracketing the line (Worthey et al. 1994).

Known the index for a single star, we weight its contribution to the integrated value on the relative number of stars of the same type. Therefore the integrated index is given by

$$I_1^{\text{SSP}} = \Delta_\lambda \left(1 - \frac{\sum_i F_{1,i}^* N_i}{\sum_i F_{c,i}^* N_i} \right) \quad \text{in EW} \quad (15)$$

$$I_1^{\text{SSP}} = -2.5 \log \left(\frac{\sum_i F_{1,i}^* N_i}{\sum_i F_{c,i}^* N_i} \right) \quad \text{in Mag}$$

where N_i is the number of stars of type i -th.

When computing actual SSPs, single stars are identified to the isochrone elemental bins defined in such a way that all relevant quantities, i.e. luminosity, T_{eff} , gravity, and mass vary by small amounts. In particular, the number of stars per isochrone bin is given by

$$N_i = \int_{m_a}^{m_b} \phi(m) dm \quad (16)$$

where m_a and m_b are the minimum and maximum star mass in the bin and $\phi(m)$ is the mass function in number.

Indicating $F_{1,i}^* N_i$ and $F_{c,i}^* N_i$ with $\mathcal{F}_{1,i}^*$ and $\mathcal{F}_{c,i}^*$, respectively, the eqns. (15) can be written as

$$I_1^{\text{SSP}} = \Delta_\lambda \left(1 - \frac{\sum_i \mathcal{F}_{1,i}^*}{\sum_i \mathcal{F}_{c,i}^*} \right) \quad \text{in EW} \quad (17)$$

$$I_1^{\text{SSP}} = -2.5 \log \left(\frac{\sum_i \mathcal{F}_{1,i}^*}{\sum_i \mathcal{F}_{c,i}^*} \right) \quad \text{in Mag}$$

These are the equations adopted to calculate the indices of SSPs.

However, in order to evaluate the contribution to the total value of an index by stars of the same SSP but in different evolutionary stages, it is convenient to recast eqns. (17) in a slightly different way. Naming $\mathcal{I}_{1,i}^*$ the mean index of the isochrone bin, using eqns. (14), and applying simple algebraic manipulations, eqns. (17) become

$$I_1^{\text{SSP}} = \frac{\sum_i \mathcal{F}_{c,i}^* \mathcal{I}_{1,i}^*}{\sum_i \mathcal{F}_{c,i}^*} = \sum_i f_{c,i}^* \mathcal{I}_{1,i}^* \quad \text{in EW}$$

$$I_1^{\text{SSP}} = -2.5 \log \left(\frac{\sum_i \mathcal{F}_{c,i}^* 10^{-0.4\mathcal{I}_{1,i}^*}}{\sum_i \mathcal{F}_{c,i}^*} \right) \quad (18)$$

$$= -2.5 \log \left(\sum_i f_{c,i}^* 10^{-0.4\mathcal{I}_{1,i}^*} \right) \quad \text{in Mag}$$

where $f_{c,i}^* = \mathcal{F}_{c,i}^* / \sum_i \mathcal{F}_{c,i}^*$ (or $f_{c,i}^* = \mathcal{F}_{c,i}^* / \mathcal{F}_{c,i}^{\text{SSP}}$) is the contribution of the stars in each isochrone bin to the total pseudo-continuum flux of the SSP. The same notation of eqns. (18) can be used to indicate the j -th evolutionary phase and to evaluate the contribution of this to the building up of a generic index (see Section 8.1 below).

5 α -ENHANCED INDICES

The *Fitting Functions* are one of the most crucial issues of the whole problem because it is long known that a great deal

of the final results actually depend on them. In the following we shortly summarize the most popular ones and then make our final choice.

5.1 The Worthey Fitting Functions

The widely used *Fitting Functions* by Worthey et al. (1994) (see also Worthey & Ottaviani 1997) depend only on T_{eff} , gravity, and $[\text{Fe}/\text{H}]$. Therefore the effect of an α -enhanced chemical composition will act only via the decrease in $[\text{Fe}/\text{H}]$ given by eqn. (4) whereas the *Fitting Functions* themselves will be insensitive to the abundances of the enhanced elements but for the rescaling of $[\text{Fe}/\text{H}]$. Therefore, they provide only a minimum effect of an α -enhanced composition.

In contrast, many studies have emphasized that absorption line indices should also depend on the detailed pattern of chemical abundances (Barbuy 1994; Idiart & de Freitas-Pacheco 1995; Weiss et al. 1995; Borges et al. 1995). To cope with this problem two ways out are available: the empirical *Fitting Functions* by Borges et al. (1995) and the semi-theoretical *Response Functions* by Tripicco & Bell (1995). Unfortunately, the *Fitting Functions* by Borges et al. (1995) are limited to Mg_2 and NaD . For all the other indices one has to make use of the Worthey et al. (1994) *Fitting Functions*. Since they are insensitive to α -enhanced but for the different $[\text{Fe}/\text{H}]$, a great deal of the potential effect of enhancing the α -elements is lost.

5.2 The Tripicco & Bell (1995) method

A method designed to include the effects of enhancement on all indices at once has been suggested by Tripicco & Bell (1995, TB95), who introduce the concept of *Response Functions*. In brief from model atmospheres and spectra for three proto-type stars, i.e. a Cool-Dwarf star (CD) with $T_{\text{eff}}=4575$ K and $\log(g)=4.6$, a Turn-Off (TO) star with $T_{\text{eff}}=6200$ K and $\log(g)=4.1$, and a Cool-Giant (CG) star with $T_{\text{eff}}=4255$ K and $\log(g)=1.9$, they calculate the absolute indices I_0 . Doubling the abundances X_i of the C, N, O, Mg, Fe, Ca, Na, Si, Cr, and Ti in steps of $\Delta[X_i/\text{H}]=0.3$ dex they determine the incremental ratios $\Delta I_0/\Delta[X_i/\text{H}]$ in units of the observational error σ_0 . The absolute indices I_0 , the observational error σ_0 , and the normalized incremental ratios δI_0 are given in Tables 4, 5 and 6 of TB95. The true incremental ratios are $\Delta I_0/\Delta[X_i/\text{H}]0.3 = \delta I_0 \times \sigma_0$. The *Response Functions* $R_{0.3}(i)$ for any index corresponding to the variation of the element i -th $\Delta[X_i/\text{H}] = +0.3$ dex, is given by

$$R_{0.3}(i) = \frac{1}{I_0} \frac{\Delta I_0}{\Delta[X_i/\text{H}]} 0.3$$

The *Response Functions* for Cool-Dwarfs, Cool-Giants, and Turn-Off stars constitute the milestones of the calibration. They are used to correct the indices for solar partitions (Worthey et al. 1994) in presence of α -enhancement.

The technical methods for correcting an index from solar to α -enhanced element partitions have been proposed by TFWG00 and TMB03. Since the two methods are not strictly equivalent, some clarification is worth here.

Without providing a formal justification, TFWG00 propose that the fractional variation of an index to changes of the

chemical parameters is the same as that for the reference index I_0 according to the relation

$$\frac{\Delta I}{I} = \frac{\Delta I_0}{I_0} = \left\{ \prod_i [1 + R_{0.3}(i)]^{\frac{[X_i/\text{H}]}{0.3}} \right\} - 1 \quad (19)$$

where $R_{0.3}(i)$ are the *Response Functions* tabulated by TB95 (in view of the discussion below we call attentions on the negative values for some I_0 in their list). Relation (19) can be derived as follows. We start from the assumption that

$$\frac{dI}{I} = \text{const}, \quad (20)$$

differentiate the generic index I with respect to the abundance ratios

$$dI_0 = \sum_i \frac{\partial I_0}{\partial [X_i/\text{H}]} 0.3 \frac{d[X_i/\text{H}]}{0.3} \quad (21)$$

and write

$$\frac{dI_0}{I_0} = \sum_i r_{0.3}(i) \frac{d[X_i/\text{H}]}{0.3} \quad (22)$$

where $r_{0.3}(i) = \frac{1}{I_0} \frac{\partial I_0}{\partial [X_i/\text{H}]} 0.3$. We have introduced the quantity $r_{0.3}(i)$ containing the partial derivatives to distinguish it from the *Response Functions* $R_{0.3}(i)$ defined above. Integrating relation (22) we obtain

$$\ln|I| = \ln|I_0| + \sum_i r_{0.3}(i) \frac{[X_i/\text{H}]}{0.3} \quad (23)$$

which upon exponentiation becomes

$$I = I_0 \prod_i \exp[r_{0.3}(i)]^{\frac{[X_i/\text{H}]}{0.3}} \quad (24)$$

with the obvious condition that $I/I_0 > 0$. Recalling that TB95 provide the ratio $\frac{\Delta I_0}{\Delta[X_i/\text{H}]}$ evaluated for $\Delta[X_i/\text{H}]=0.3$, for each chemical element we may write

$$\left(\frac{1}{I_0} \frac{\Delta I_0}{\Delta[X_i/\text{H}]} \right)_i = \frac{1}{I_0} \frac{I_0 \exp[r_{0.3}(i)] - I_0}{0.3} \quad (25)$$

from which we derive

$$\exp[r_{0.3}(i)] = 1 + \left(\frac{1}{I_0} \frac{\Delta I_0}{\Delta[X_i/\text{H}]} 0.3 \right)_i = 1 + R_{0.3}(i) \quad (26)$$

Substituting the $\exp[r_{0.3}(i)]$ into relation (24) and performing trivial algebraic manipulations we obtain the relation (19) of TFWG00, with the only condition that $R_{0.3}(i) > -1$. The advantage of this formulation is that no particular constraint is required on the sign of I_0 and the incremental ratios given by TB95 are straightforwardly used. As a final remark, relation (19) implies that the per cent change is constant for each step of 0.3 dex. However, as emphasized by TFWG00, eqn. (19) while securing that the indices tend to zero for small abundances it let them increase with the exponent $[X_i/\text{H}]/0.3$. For abundances higher than

Table 3. Fractional variations $\Delta I/I$ of the indices of the milestone stars of the TB95 calibration for the α -enhanced mixtures adopted in this study.

Indices	$\Gamma = 0.35$			$\Gamma = 0.50$			
	Cool-Dwarf	Cool-Giants	Turn-Off	Cool-Dwarf	Cool-Giants	Turn-Off	
1	CN ₁	-0.86877	-0.71770	0.06423	-0.94202	-0.83719	0.09355
2	CN ₂	-0.70699	-0.64130	0.12677	-0.83117	-0.77143	0.18661
3	Ca4227	0.49139	1.16619	0.29979	0.75632	1.96846	0.42250
4	G4300	-0.21532	-0.22310	-0.21811	-0.30403	-0.30946	-0.30218
5	Fe4383	-0.30258	-0.23803	-0.37851	-0.40260	-0.32100	-0.50678
6	Ca4455	0.10268	0.21885	-0.16305	0.15128	0.32776	-0.22517
7	Fe4531	0.11746	0.00750	-0.08348	0.15334	-0.00689	-0.13409
8	C ₂ 4668	-0.86323	-0.74107	-0.75182	-0.94322	-0.85574	-0.87089
9	H _{β}	3.84438	-	0.02082	7.23898	-	0.02685
10	Fe5015	-0.00723	-0.03527	-0.00808	-0.02139	-0.05729	-0.00496
11	Mg ₁	-0.05511	-0.40093	-0.39931	-0.10092	-0.53182	-0.52801
12	Mg ₂	0.01540	-0.00348	-0.00323	0.00611	-0.02029	-0.02536
13	Mg _b	0.17517	0.89365	0.32348	0.24424	1.48472	0.49262
14	Fe5270	-0.13515	-0.20974	-0.08969	-0.19210	-0.28893	-0.15437
15	Fe5335	-0.18802	-0.11060	-0.26476	-0.26154	-0.15684	-0.37135
16	Fe5406	-0.21219	-0.20857	-0.41037	-0.29123	-0.28739	-0.55194
17	Fe5709	0.07110	0.15444	-0.14799	0.09688	0.22449	-0.22470
18	Fe5782	-0.21869	-0.17021	-0.59314	-0.30428	-0.23570	-0.74622
19	NaD	-0.18801	-0.29678	-0.49855	-0.26211	-0.40124	-0.65122
20	TiO ₁	0.00000	-0.76789	0.01280	0.00000	-0.87503	0.11905
21	TiO ₂	-0.33456	-0.55618	-0.26927	-0.44872	-0.69355	-0.36565

$[X_i/H] = +0.6$ dex, the exponent may become too large and consequently the correction may diverge.

A different reasoning has been followed by TMB03. In brief, they start from the observational hint that in Galactic stars $Mg_2 \propto \exp([Mg/H])$ (see Borges et al. 1995), to assume that all indices depend exponentially on the abundance ratios, introduce the variable $\ln I \propto [X_i/H]$, and express the fractional variation of an index to changes in the abundance ratios as

$$\frac{\Delta I}{I} = \left\{ \prod_i \exp(R_{0.3}(i)) \frac{[X_i/H]}{0.3} \right\} - 1 \quad (27)$$

Although the exponential term in (27) may look like to that of eqn. (24) actually they do not because the partial derivatives, i.e. the term $r_{0.3}(i)$, are replaced by the response functions $R_{0.3}(i)$.

As general remark, the use of eqns. (19) and (27) requires that the sign of the index to be corrected is the same of the corresponding I_0 in TB95. In general this holds good. In principle, it may, however, happen that the signs do not coincide. To overcome this potential difficulty, TMB03 apply a correcting procedure forcing the negative reference indices I_0 of TB95 to become positive. This occurs in particular for H_β of Cool-Dwarf stars (and others as well). The argument is that TB95 neglecting non-LTE effects underestimate the true values of H_β so that negative values found for temperatures lower than about 4500 K should be shifted to higher, positive values (see Fig.12 in TB95). Although we may agree on this issue, we suspect that any change to the values tabulated by TB95 may be risky for a number of reasons: (i) The *Fitting Functions* have been derived from a set of data that include a significant number of stars with negative values of H_β ; (ii) The incremental ratios by TB95 have been calculated for particular stars (stellar spectra) with assigned T_{eff} , $\log(g)$, and I_0 . Changing the reference I_0 while leaving

unchanged the incremental ratios (partial derivatives) may not be very safe. The ideal approach would be to repeat the TB95 analysis using different samples of data and baseline spectra; (iii) The replacement of the partial derivatives with the TB95 incremental ratios may be risky when dealing with exponential functions; (iv) The large corrections required to shift the I_0 for a number of indices; (v) Finally, the use of $\ln I$ as dependent variable which requires that only positive values for I_0 are considered.

In any case, to proceed further, one has to fix the abundance of those α -elements that are enhanced with respect to the solar partition. With the abundances specified in Tables 1 and 2 and the TFWG00 method (eqn. (19) above) we calculate the relative variations $\Delta I/I$ for each index of the Worthey et al. (1994) system for the milestone stars of the TB95 calibration. The results are summarized in Table 3 for $\Gamma=0.35$ and $\Gamma=0.50$. To avoid misunderstanding, it is worth calling attention that the quantities listed in Table 3 are the total relative variations to changing all chemical abundances at once, and not the response to changing individual species. Several remarks are worth here: firstly adopting the TMB03 procedure the resulting $\Delta I/I$ are different and in some cases cannot be even calculated; secondly comparing our $\Delta I/I$ with those evaluated by TMB03, in particular for some crucial elements like H_β , these latter turn out to be significantly smaller than ours because of the increase of I_0 at constant $\Delta I_0/\Delta[X_i/H]$ (see above) adopted by TMB03. This will reflect on the nearly constant H_β at increasing enhancement they have found. Finally, the fractional variation for the H_β index in Cool-Giant stars cannot be defined. Neither relation (19) nor relation (27) can be used, because the index has changed sign with respect to I_0 . However, since in any case the contribution from this type of stars to the total value for an SSP will be small we simply neglect the correction.

Is there any independent argument favoring one cor-

Table 4. Indices and their variations from Tripicco & Bell (1995) and Tantalo et al. (2004) using the new library of high resolution spectra by Munari et al. (2004). I_0 always denotes the value of the index for the solar-scaled compositions, whereas $I_{(M/H)}$ is the value obtained by increasing the α -elements by +0.3 dex in Tripicco & Bell (1995) and +0.4 dex in Tantalo et al. (2004). The selected stars are the same as in Tripicco & Bell (1995), whereas in the case indicated as “1 Å resolution spectra” these are the closest matches in T_{eff} and $\log(g)$ in the library to our disposal. The metallicity is always solar. See the text for more details.

		Tripicco & Bell (1995)			1 Å Resolution Spectra		
Index		CD	TO	CG	CD	TO	CG
	T_{eff}	4575	6200	4255	4500	6200	4200
	$\log(g)$	4.6	4.1	1.9	4.5	4.0	2.0
C ₂ 4668	I_0	2.340	0.770	8.620	2.650	1.125	3.705
	$I_{(M/H)}$	3.044	1.794	11.180	4.500	0.800	4.000
	$\Delta I/I$	0.300	1.329	0.297	0.698	-0.289	0.079
H_β	I_0	-0.100	3.790	0.050	0.350	4.000	0.100
	$I_{(M/H)}$	-0.254	3.900	-0.038	0.900	5.000	0.550
	$\Delta I/I$	1.540	0.030	-1.760	1.571	0.250	4.450
Mg ₂	I_0	0.530	0.070	0.360	0.520	0.120	0.456
	$I_{(M/H)}$	0.568	0.083	0.409	0.610	0.130	0.605
	$\Delta I/I$	0.072	0.186	0.130	0.360	0.083	0.327

recting method against the other? Firstly, in addition to the response for separate enhancements by 0.3 of individual species, TB95 also provide the response to increasing all the “metals” at once by the same factor. The resulting indices (limited to a few illustrative cases and shortly indicated as $I_{(M/H)}$) are reported in the columns labelled “Tripicco & Bell (1995)” of Table 4, They should provide a sort of upper limit to the expected correction. Secondly, basing on the huge library of 1 Å resolution synthetic spectra calculated by Munari et al. (2004) over a large range of $\log T_{\text{eff}}$, $\log(g)$, $[\text{Fe}/\text{H}]$ and both for solar and α -enhanced abundance ratios ($[\text{X}_{\text{el}}/\text{Fe}]$), Tantalo et al. (2004) have derived theoretical line absorption indices on the Lick system. The α -enhanced mixture is obtained by increasing at once the abundance ratios $[\text{X}_{\text{el}}/\text{Fe}]$ by 0.4 for O, Mg, Si, S, Ca, Ti, many of which are in common with the present list. This is the analog of the case “all metals at once” of Tripicco & Bell (1995). In the following we will make use of these results in advance of publication to evaluate I_0 and $I_{(M/H)}$ and the ratio $\Delta I/I$. The results are presented in the three columns of Table 4 labelled “1 Å Resolution Spectra”. Comparing the three groups of data for $\Delta I/I$ (i.e. those of Table 3, those of the TB95 all metals enhanced at once, and those from the 1 Å resolution synthetic spectra) the situation is as follows: all the three agree on H_β and marginally for Mg₂, whereas they disagree on C₂4668.

Since a great deal of the discussion below depends on the response of H_β to Γ and also to the abundance ratios adopted for some elements at given Z and Γ , it is worth commenting on the reason why we expect H_β to increase with Γ and/or $[\text{X}_{\text{el}}/\text{Fe}]$. The effect on other indices is less of a problem. To this aim, with the aid of the Munari et al. (2004) 1 Å resolution spectra and the results by Tantalo et al. (2004), limited to the case of a typical cool-giant with $T_{\text{eff}}=4000$ K, $\log(g)=4.5$, and $[Z/Z_\odot]=-0.5$ ($Z=0.008$), in Fig. 1 we show how the index H_β is built up and how it varies passing from $[\alpha/\text{Fe}]=0.0$ to $[\alpha/\text{Fe}]=+0.4$. Firstly in the bottom panel we display the ratio $F_{\lambda,\text{enh}}/F_{\lambda,\odot}$ and the pass-bands defining the index H_β . The absorption in the α -enhanced spectrum is significantly larger than the solar-scaled one. The effect is larger in the blue pseudo-continuum and central band than

in the red pseudo-continuum. This means that α -enhanced mixtures distort the spectrum in such a way that simple predictions cannot be made. This is due to the contribution of many molecular bands and atomic lines of elements like C, N, O, Mg, Ti, falling in the spectral regions of interest. Secondly, in the upper panel we show the spectral energy distribution of the solar-scaled (solid line) and α enhanced (dotted line) spectrum and once more the pass-bands for H_β . The open circles and star shows the mean fluxes in the three pass-band and the interpolation of the pseudo-continuum to derive F_c in the case of solar-scaled spectrum. The filled triangles and pentagon are the same but for the α -enhanced mixture. The increase of H_β passing from solar to α -enhanced abundance ratios is straightforward.

Even if the ideal situation would be to replace the old *Response Functions* of TB95 with new ones derived from modern high resolution spectra, this indeed is the main target of Tantalo et al. (2004), given that the TFWG00 algorithm has been proved to be of general validity, to safely use the incremental ratios of TB95, and to give results in agreement with those from high resolution spectra, for the purposes of the present study we prefer to use the TB95 *Response Functions* combined with the TFWG00 algorithm for the sake of consistency with results by other authors on the same subject. Finally, it is also easy to check that the same results of TFWG00 and TMB03 are recovered when the same set of chemical parameters are adopted (see the Table 5 of TFWG00 and the discussion in Sect. 9.6 below). It is worth recalling, however, that the final results will somewhat depend on which correcting technique is adopted. This is a point to keep in mind deserving further investigation.

Once the fractional variations of the milestone stars, $(\Delta I/I)_{\text{CD}}$, $(\Delta I/I)_{\text{TO}}$, and $(\Delta I/I)_{\text{CG}}$ respectively, are known, they are linearly interpolated both in $\log(g)$ and $\log T_{\text{eff}}$ to get the total fractional variation $(\Delta I/I)$ to be applied to the solar-scaled indices for each elemental bin of an isochrone while performing the integration along it. The double interpolation scheme assigns different weights to the calibrators according to their distance with respect of the current elemental bin in the HR-Diagram. The dependence of the fractional variations on gravity and effective temperature is

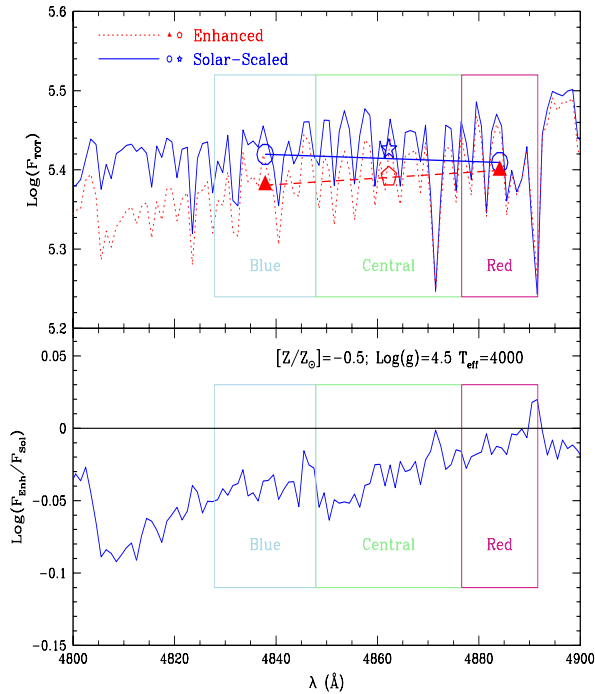


Figure 1. Building-up of the index H_β in the cool dwarf with $T_{\text{eff}}=4000$ K, $\log(g)=4.5$, and $[Z/Z_\odot]=-0.5$ both for the solar-scaled and the pattern of abundance ratios with $[\alpha/\text{Fe}]=+0.4$. The bottom panel shows the ratio $F_{\lambda,\text{enh}}/F_{\lambda,\odot}$. The absorption in the α -enhanced spectrum is significantly larger than the solar-scaled one. The effect is larger in the blue wing of the pseudo-continuum and central band than in the red pseudo-continuum. Upper panel the spectral energy distribution of the solar-scaled (solid line) and α enhanced (dotted line) spectrum and the pass-bands defining the index H_β . The open circles and star shows the mean fluxes in the three pass-band and the interpolation of the pseudo-continuum to derive F_c in the case of solar-scaled spectrum. The filled triangles and pentagon are the same but for the α -enhanced mixture. The increase of H_β passing from solar to α enhanced abundance ratios is obvious.

imposed by the TB95 study. Having only three stars as calibrators, no other procedure can be found to account for the change of the fractional variations along an isochrone. As a consequence of it, as the age increases and the isochrone TO shifts to lower T_{eff} and higher gravities, the relative weight of CD stars (for some indices they often have the highest *Response Functions*) on determining the total *Response Function* gets higher. This is an additional cause of the sensitivity of indices such as H_β to the fractional variations.

6 BUILDING THE INDICES OF SSPS

In this study we will make use only of the TB95 calibration both for the sake of brevity and because we intend to compare our results with those by TFWG00 who adopted the same transformation. With the aid of the SGWC00 SSPs, the pattern of abundances and abundance ratios presented in Tables 1 and 2, and the TB95 calibrations and its companion corrections listed in Table 3, we finally derive the whole

set of indices on the Lick System for SSPs of different age, metallicity and Γ . To apply the TB95 corrections we proceed as follows: for each elemental bin of an isochrone and/or SSP with assigned Γ , we derive the index according to the *Fitting Functions* and correct it according to eqn. (19) by interpolating the entries of Table 3 as appropriate to the current values of T_{eff} , and gravity (luminosity class), and follow the whole procedure described in Section 4. Extensive tabulations of the complete set of the Lick System for SSPs of different age, metallicity ($Z=0.008, 0.019, 0.040$, and 0.070) and Γ ($0, 0.35$ and 0.5) are available from the authors and the web site <http://dipastro.pd.astro.it/galadriel>.

To illustrate the results we show in Fig. 2 the temporal evolution of eight important indices, i.e. Mg_b , Mg_2 , H_β , $\langle\text{Fe}\rangle$, $[\text{MgFe}]$, $[\text{MgFe}]'$, NaD and C_24668^3 , for the following combinations of metallicity and Γ , namely $Z=0.008$ (solid lines) and $Z=0.070$ (broken lines), $\Gamma=0$ (heavy lines) and $\Gamma=0.35$ (thin lines). The age goes from 0.01 Gyr to 20 Gyr.

The merit of this set of indices is the internal consistency as far as the chemical parameters are concerned. The stellar models and the indices have been calculated with the same pattern of abundances.

All indices show the same behavior. For ages older than about 3 Gyr they all tend to flatten out (*age-degeneracy*). In order to quantify the response of the indices to changes in metallicity Z , enhancement factor Γ , and age T we calculated the relative per cent variations

$$\left[\frac{\Delta I}{I}\right]_{Z,\Gamma} \quad \left[\frac{\Delta I}{I}\right]_{T,\Gamma} \quad \text{and} \quad \left[\frac{\Delta I}{I}\right]_{T,Z}$$

where I stands for the generic index, and the variations ΔI are calculated for $\Delta Z=0.070-0.008=0.062$, $\Delta T=15-5=10$ Gyr, and $\Delta \Gamma=0.35$. The per cent variations are evaluated at fixed values of metallicity ($Z=0.008$ and 0.070), total enhancement factor ($\Gamma=0$ and 0.35), and age ($T=5, 10$ and 15 Gyr) as appropriate. The results are summarized in Table 5 for the eight indices shown in Fig. 2. These evaluations can be easily extended to any index of the Worthey et al. (1994) list. It is soon clear that C_24668 and NaD strongly depend on metallicity and to a lesser extent on Γ , whereas they scarcely depend on the age. The indices $[\text{MgFe}]$ and $[\text{MgFe}]'$ are almost insensitive to Γ in agreement with TMB03. All remaining indices almost evenly depend on the three parameters with little resolving power. Finally, there is a non negligible dependence on the total metallicity Z for some of the indices (H_β in particular).

³ The definition of $\langle\text{Fe}\rangle$, $[\text{MgFe}]$ and $[\text{MgFe}]'$ is

$$\langle\text{Fe}\rangle = 0.5 \times (\text{Fe}5270 + \text{Fe}5335)$$

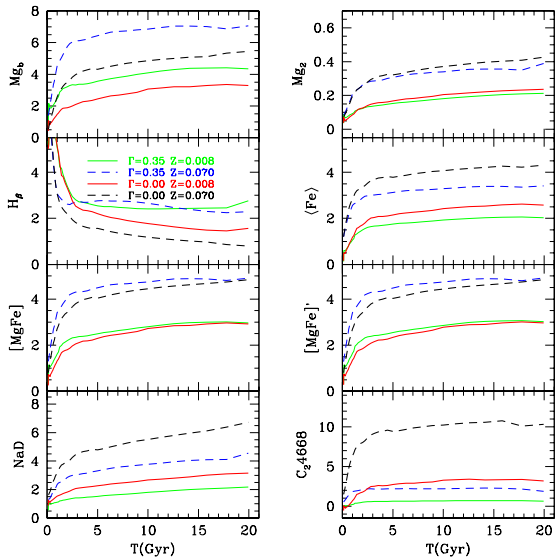
$$[\text{MgFe}] = \sqrt{\text{Mg}_b \times (0.5 \times \text{Fe}5270 + 0.5 \times \text{Fe}5335)}$$

and

$$[\text{MgFe}]' = \sqrt{\text{Mg}_b \times (0.72 \times \text{Fe}5270 + 0.28 \times \text{Fe}5335)}$$

Table 5. Relative per cent variations of the indices at changing age, metallicity, and Γ . The indices are for the SSPs of SGWC00 with $\Gamma=0$ and $\Gamma=0.35$.

T(Gyr)	ΔZ	Γ	ΔH_β	$\Delta[MgFe]$	$\Delta[MgFe]'$	$\Delta\langle Fe \rangle$	ΔMg_b	ΔMg_2	ΔNaD	ΔC_24668
5.00	0.06	0.00	-29 %	76 %	72 %	76 %	76 %	91 %	111 %	245 %
10.00	0.06	0.00	-34 %	63 %	60 %	68 %	58 %	81 %	107 %	210 %
15.00	0.06	0.00	-35 %	60 %	57 %	65 %	55 %	76 %	103 %	223 %
5.00	0.06	0.35	8 %	80 %	76 %	79 %	81 %	101 %	118 %	258 %
10.00	0.06	0.35	10 %	69 %	66 %	71 %	68 %	88 %	109 %	225 %
15.00	0.06	0.35	-6 %	63 %	60 %	66 %	59 %	74 %	99 %	225 %
T(Gyr)	Z	$\Delta\Gamma$	ΔH_β	$\Delta[MgFe]$	$\Delta[MgFe]'$	$\Delta\langle Fe \rangle$	ΔMg_b	ΔMg_2	ΔNaD	ΔC_24668
5.00	0.008	0.35	16 %	9 %	9 %	-19 %	45 %	-10 %	-33 %	-78 %
10.00	0.008	0.35	36 %	3 %	3 %	-21 %	33 %	-12 %	-32 %	-79 %
15.00	0.008	0.35	64 %	3 %	3 %	-21 %	33 %	-10 %	-32 %	-79 %
5.00	0.070	0.35	76 %	11 %	11 %	-17 %	49 %	-5 %	-31 %	-77 %
10.00	0.070	0.35	124 %	7 %	7 %	-19 %	41 %	-8 %	-32 %	-79 %
15.00	0.070	0.35	136 %	4 %	5 %	-20 %	37 %	-11 %	-33 %	-79 %
ΔT (Gyr)	Z	Γ	ΔH_β	$\Delta[MgFe]$	$\Delta[MgFe]'$	$\Delta\langle Fe \rangle$	ΔMg_b	ΔMg_2	ΔNaD	ΔC_24668
10.00	0.008	0.00	-32 %	27 %	27 %	20 %	34 %	36 %	33 %	22 %
10.00	0.070	0.00	-38 %	16 %	16 %	13 %	18 %	25 %	28 %	14 %
10.00	0.008	0.35	-4 %	20 %	20 %	17 %	24 %	35 %	35 %	14 %
10.00	0.070	0.35	-17 %	9 %	9 %	8 %	9 %	16 %	23 %	3 %

**Figure 2.** Evolution of eight indices (Mg_b , Mg_2 , H_β , $\langle Fe \rangle$, $[MgFe]$, $[MgFe]'$, NaD and C_24668) as function of the age. The heavy lines show the indices for solar-scaled partition of elements ($\Gamma=0$), whereas the thin lines show the same but for the partition of α -enhanced of SGWC00 ($\Gamma=0.35$). Only two metallicities are displayed for the sake of clarity, i.e. $Z=0.008$ (solid lines) and $Z=0.07$ (dashed lines).

7 GALAXY AGES, METALLICITIES AND ABUNDANCE RATIOS

7.1 Which indices to choose?

As already mentioned above, the ultimate scope of a system of indices is to derive the age, metallicity, and enhancement factor of the stars in aggregates of different complexity going from clusters to galaxies, the EGs in particular. To proceed further in the analysis one has to find three or more indices, or combination of these, most sensitive to the parameters in

question. It commonly thought that indices like H_β are good age indicators, whereas others like Mg_b , $\langle Fe \rangle$, Mg_2 are good metallicity indicators. However, the results presented in the previous sections and the discussion below will clarify that a certain degree of degeneracy among the different parameters is always present so that there is no clear one to one dependence of an index from age, metallicity and degree of α -enhancement.

Furthermore, the choice is often dictated by the available databases of indices. Among others, the most popular databases are the catalogs by González (1993) for nearby field early-type galaxies, and the Trager “*IDS Pristine*” sample (see Trager 1997, Table 3.1) for the central regions of elliptical galaxies. For the purposes of the present study, the analysis will be limited to these samples of data, leaving aside for the time being other more recent compilations. The González (1993) catalog provides H_β , the iron-group indices, and the Mg-group indices for the region within the radius $R_{\text{eff}}/8$ for a sample of nearby field galaxies. The Trager (1997) sample lists H_β , the higher-order Balmer line indices ($H_{\delta A}$, $H_{\gamma A}$, $H_{\delta F}$, $H_{\gamma F}$), the iron-peak indices, C_24668 , and others. We adopt here the indices H_β , $\langle Fe \rangle$, Mg_2 , Mg_b , NaD and C_24668 on which much work has been done in the past so that the comparison is possible.

7.2 The Minimum-Distance method

As already proposed by TFWG00 the so-called *Minimum-Distance Method* is perhaps best suited to our purposes. Suppose that a galaxy and/or a star cluster is characterized by a set of observationally measured indices $I_{i,\text{obs}}$, from which we want to infer the age, the metallicity Z , and the degree of α -enhancement Γ . On the theoretical side, suppose we have the corresponding indices tabulated as a function of the same quantities in form of discrete grids of values $I_{i,\text{th}}(t_j, Z_k, \Gamma_l)$ where j , k , and l vary from 1 to a certain value as appropriate. In the space of the indices I_i we define the distance between the observational set $I_{i,\text{obs}}$ and a generic point of the correspondent space $I_{i,\text{th}}$:

$$D = \left[\sum_i (I_{i,\text{th}} - I_{i,\text{obs}})^2 \right]^{0.5} \quad (28)$$

By varying $I_{i,\text{th}}$ over the whole grid space we find the particular triplet j, k, l for which D is minimal. This means to fix the age, metallicity Z , and Γ .

There are two points of concern with the *Minimum-Distance Method*. Firstly, as pointed out by Buzzoni (2004, private communication), not all indices are expressed in the same units: some are in equivalent width others in magnitudes, which poses a physical inconsistency regarding the distance in such multi-dimensional space. Furthermore even in the case of homogeneous indices, their absolute values may greatly differ. It would be better to re-scale all indices to some suitable units: for instance the variance or the mean values of the observational sample they are applied to, or the intrinsic accuracy. In the following we will apply the method as it is, in order to be able to compare our results with TFWG00. Work is currently underway to revise the *Minimum-Distance procedure* (Tantalo & Chiosi 2004a, in preparation). Secondly the method is safe in the case of the star clusters because their stellar content is well mimicked by a SSP. In real galaxies, the situation is more complicate and risky because even in the case of EGs a mix of stellar populations with different age and chemical properties is likely to exist. Therefore the approximation to SSP is no longer valid and SSPs should be replaced by galactic models incorporating the history of star formation and chemical enrichment and the indices to be used should take into account the contribution from all stellar components. Integrated indices for model galaxies have been calculated by Tantalo et al. (1998) but never applied to this kind of analysis. Despite this, since most if not all of the studies in literature are based on the SSP approximation, we will adopt it also here.

To be applied the *Minimum-Distance Method* requires large grids of SSPs with fine spacing in age, metallicity and Γ . The SGWC00 grids of SSPs cover a wide age range with narrow spacing, and span a large range in metallicity, $0.008 \leq Z \leq 0.070$. Thanks to their regular behavior over large ranges of age and metallicity additional SSPs can be added by interpolation. However, the grids are only for $\Gamma=0$ and $\Gamma=0.35$. The simple extrapolation to higher values of Γ may be risky, because of the non linear response of the calibration to variations of this important parameter. To cope with this problem without embarking in the tedious and time consuming calculations of new grids of stellar models with higher degree of α -enhancement, the following strategy has been adopted. The detailed stellar model calculations by SGWC00 have shown that keeping constant all other physical parameters passing from $\Gamma=0$ to 0.35 or equivalently re-scaling $[\text{Fe}/\text{H}]$ as appropriate, the stellar models by themselves do not change in a dramatic fashion but for expected effects due to the lower $[\text{Fe}/\text{H}]$ and the higher $[\alpha/\text{Fe}]$ that can be easily handled. Taking advantage of it, firstly we prepare a new pattern of chemical abundances having $\Gamma=0.50$ by extrapolating the variations in individual species passing from $\Gamma=0$ to 0.35 according to the recipe by SGWC00. These have already been shown in Tables 1 and 2. Secondly, using the SSPs by SGWC00 we calculate new grids of indices

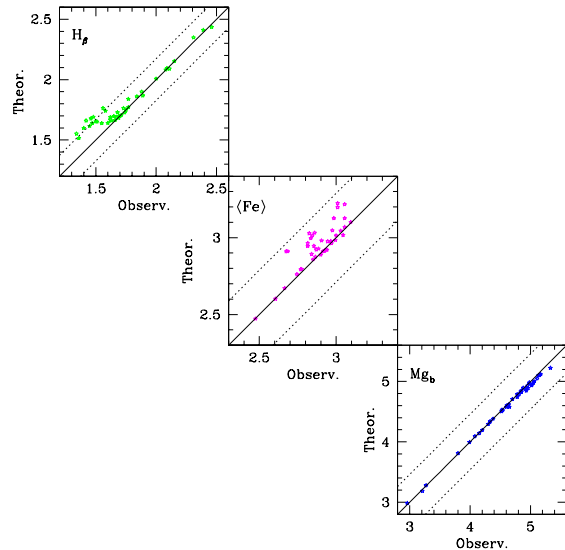


Figure 3. Quality test for the indices H_β , Mg_b , $\langle \text{Fe} \rangle$. The theoretical value is plotted against the observational one. All indices pass the quality test as the theoretical observational values coincide within the uncertainty of 10%.

with the new pattern of abundances for $\Gamma=0.50$. Finally, we generate the large grid of SSPs suited to the *Minimum-Distance Method*. The grids span the ranges $0 \leq T \leq 20$ Gyr, $0.008 \leq Z \leq 0.070$ or $-0.40 \leq [\text{Z}/\text{H}] \leq 0.68$, and $0 \leq \Gamma \leq 0.50$. The age spacing is the same as in the SGWC00 database of isochrones. For the metallicity, by adopting $Z_\odot=0.019$ and $X_\odot=0.708$, we replace the abundance by mass Z with $[\text{Z}/\text{H}]$ so that the results can be immediately compared to those by TFWG00. The spacing in metallicity is $\Delta[\text{Z}/\text{H}] = 0.022$. Finally, Γ is spaced by $\Delta\Gamma = 0.01$.

7.3 Analysis of the González sample

Using the above grid of indices, we analyze the same sample of the González (1993) catalog of EGs studied by TFWG00 and compare the results. The indices we have considered are H_β , Mg_b and $\langle \text{Fe} \rangle$. The preliminary step is to check if the three indices and the method pass the quality test, i.e. if the observational input values and the theoretical ones coincide within an uncertainty of 10%. The quality test is shown in the three panels of Fig. 3.

Fig. 4 compares the results we obtain here (upper panel) with those derived by TFWG00 for their C^0O^+ -model (central panel). More details on these models are given below. The various histograms show the fraction of galaxies $N_{\text{Gal}}/N_{\text{TOT}}$ as a function of the age in Gyr (left panel), the metallicity $[\text{Z}/\text{H}]$ (middle panels) and the enhancement factor Γ (right panels)⁴. Since the observational indices are affected by some uncertainty, i.e. $H_\beta \pm \sigma(H_\beta)$, $Mg_b \pm \sigma(Mg_b)$ and $\langle \text{Fe} \rangle \pm \sigma(\langle \text{Fe} \rangle)$, we derive the uncertainty associated to the theoretical determinations by searching the

⁴ See Section 9.2 for the correspondence between our definition of Γ and that of $[\text{E}/\text{Fe}]$ given by TFWG00.

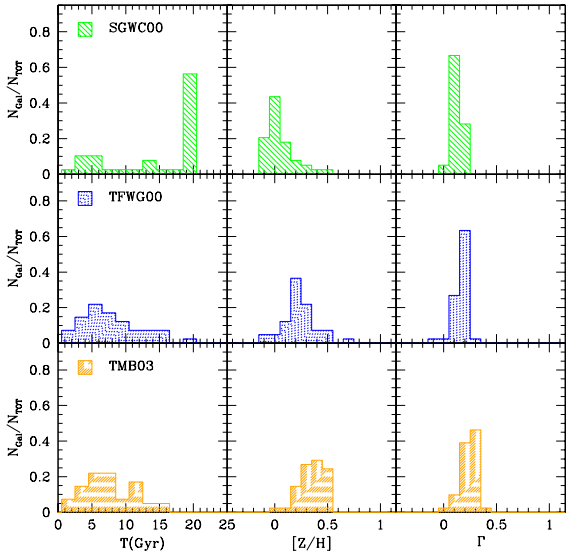


Figure 4. Distribution histograms of the age T (in Gyr), metallicity $[Z/H]$, and enhancement factor Γ (from left to right) for the galaxies in the González’s sample with $R_{\text{eff}}/8$ -aperture. The results are obtained applying the *Minimum-Distance Method* to the index-triplet H_β , Mg_b , $\langle Fe \rangle$. The top panel is for the SGWC00 models, the mid panel is for the C^0O^+ -model of TFWG00, and the bottom panel is for the TMB03 models. The last two cases are shown here for comparison.

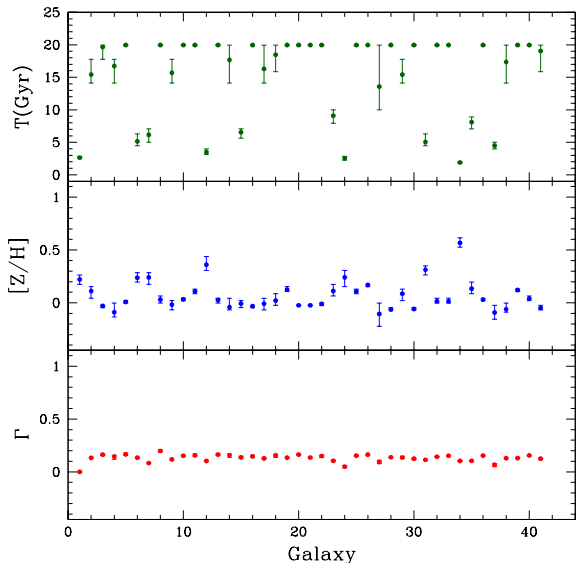


Figure 5. Analysis of the effects due to uncertainty affecting the observational indices limited to the results presented in the top panel of Fig. 4. The vertical bars show the range spanned by the age, metallicity and Γ assigned to each galaxy of the González (1993) list due to the uncertainty affecting the observational data. The x-axis is the identification number of the galaxies in the catalog. The top panel is the age T , the mid panel is the metallicity $[Z/H]$, and the bottom panel is the enhancement factor Γ .

grid at $[H_\beta \pm \sigma(H_\beta), Mg_b, \langle Fe \rangle]$, $[H_\beta, Mg_b \pm \sigma(Mg_b), \langle Fe \rangle]$, and $[H_\beta, Mg_b, \langle Fe \rangle \pm \sigma(\langle Fe \rangle)]$ and taking the maximum deviations, $\max(\Delta T)$, $\max(\Delta[Z/H])$, and $\max(\Delta\Gamma)$ as the associated uncertainties. The effect of the observational uncertainty is measured by the vertical bars on point in the three panels of Fig. 5. It is soon evident that the observational uncertainty on the indices scarcely affects the determinations of the age, metallicity, and Γ but for a few exceptions. Thanks to it, we will not carry out the analysis of the uncertainty brought about by the observational errors unless otherwise specified.

Even considering the uncertainty due to the observational “errors”, there are important differences between TFWG00’s results and ours, in particular as far as the age is concerned. While in TFWG00 the majority of galaxies have ages in the range 1 to 15 Gyr with a peak at about 6 Gyr, in our analysis the majority of galaxies turn out to be very old. The metallicity distribution peaks at $[Z/H]=0$ with a long tail up to $[Z/H]=0.5$. The peak value is about 0.25 dex lower than in TFWG00. The distributions of Γ are similar. Ours is only 0.1 dex lower than in TFWG00.

The major difficulty of the above results is with the age, because too many galaxies have the formal age of 20 Gyr, which on one hand is unacceptably too old on the other hand is the maximum value of the age grid. This simply means that the solution is poorly determined and all these cases should be discarded. Arbitrarily dropping all cases for which the age is older than 15 Gyr we are left with a handful of galaxies, whose mean age is about 5 Gyr.

Thomas & Maraston (2003) have argued that since SGWC00 α -enhanced stellar tracks are bluer than the standard ones, they yield higher H_β and weaker indices like Mg_2 , Mg_b , $\langle Fe \rangle$ etc. Based on this, TMB03 have concluded that the SGWC00 tracks lead to extremely high ages, without strong impact on metallicity and enhancement factor. Using the TMB03 grids of theoretical indices applied to the González (1993) sample, one gets the results shown in the bottom panel of Fig. 4, which are virtually indistinguishable from those of TFWG00. Once again the majority of galaxies turn out to be younger than 10 Gyr, about 30% are indeed in the age 10-16 Gyr; incidentally 15 Gyr is the age limit of the TMB03 grids. As far as the total enhancement and metallicity are concerned, the distribution of Γ peaks in the range $\Gamma \simeq 0.2-0.4$, whereas the distribution of metallicities peaks in the range $[Fe/H]=0.2$ to 0.4. In any case TMB03 SSPs yield ages that are significantly different from those of the present study.

The obvious conclusion would be that different stellar models and different chemical compositions cause the disagreement between TFWG00 and TMB03 results and ours. We suspect, however, that the reality is more complex than this simple conclusion. The suspicion arises from the similarity between TFWG00 and TMB03 despite the large difference in the input stellar models and SSPs, and the large discrepancy of our results which provide formal solutions for the age that are at the limit of the grids. It is therefore mandatory to examine the whole problem starting from its fundamentals. The analysis is split in two parts: firstly (Section 8) we will examine in detail the effects of different stellar inputs (isochrones, SSPs, etc.) and some important technical details. Secondly in Section 9 we discuss the effect of different patterns of chemical abundances that are

adopted to build, at given total metallicity Z , the total enhancement factor Γ , in other words the effect given the pattern of $[X_{ei}/Fe]$.

8 WHY SUCH BIG DIFFERENCES? THE STELLAR MODELS AND MORE

In this section we perform a systematic analysis of the effects on the absorption line indices diagnostic to assess the galaxy age, metallicity and degree of enhancement, caused by using SSPs, in which the various evolutionary phases are taken into account with different level of accuracy and completeness, by adopting different grids of theoretical indices to apply the minimum distance method, and finally by adopting different methods to correct the indices for α -enhancement.

8.1 The stellar models-isochrones and SSPs

As already mentioned, the indices of TFWG00 are based on the SSPs calculated by Worthey (1994). These latter in turn are obtained by patching together stellar models (isochrones) by Vandenberg (1985), Vandenberg & Bell (1985), Vandenberg & Laskarides (1987), and the Revised Yale Isochrones (Green et al. 1987, RYI). The Vandenberg isochrones have been extended up to the T-RGB phase using the giant branches of RYI with a number of extrapolations. As far as later stages are concerned, namely HB and AGB, they have been added by means of the Fuel Consumption Theorem of Renzini & Buzzoni (1986). See Worthey (1992) and Worthey (1994) for all details. The least we can remark is that these SSPs are a patchwork of many sources of data, which may not be fully self-consistent in all details. It is hard, if not impossible, to trace back all aspects of internal inconsistency (different physical input in the underlying stellar models, such as opacity, equation of state, mixing length parameter etc., initial chemical composition, important details of short lived phases, and finally numerical accuracy). The SSP models adopted by TMB03 and Thomas & Maraston (2003) are those of Maraston (1998) which amalgamate detailed stellar models calculations and the fuel consumption theorem (Renzini & Buzzoni 1986) to estimate the energetics of the post main sequence phases. Finally, the SSPs of SGWC00 stem from accurate evolutionary stellar models and isochrones, homogeneous in their input physics and extending up to the latest visible phases. Their net advantage is (at least) the internal consistency, which secures that no spurious effects are added to the problem.

In addition to this, in the course of our study we will occasionally use sub-sets of isochrones and SSPs of the Padova library released in different years in order to compare results based on stellar models approximately calculated with the same physics (opacity, nuclear reactions, equation of state, etc). In particular we will use the SSPs calculated by Tantalo et al. (1998,?) which are based on physical input more or less coeval to that adopted for the SSPs of Worthey et al. (1994). With respect to the classical SSPs by Bertelli et al. (1994), they differ in the mass-loss rate during the AGB phase for which the formulation by Vassiliadis & Wood (1993) was adopted. Since these SSPs have been amply described for the first time in the database for galaxy evolution models

by Leitherer et al. (1996), we will refer to them as the 1996 Tantalo's version of the Padova SSPs (TPD96).

Given these premises, it might be worth of interest (i) to assess the contribution from stars in different evolutionary phases to the total value of the SSP indices; (ii) to estimate the uncertainty in the index values caused by neglecting late evolutionary phase; (iii) to compare the TFWG00 SSPs with the closest SSPs of the Padova library; (iv) to examine in some detail the effect of core HeB and later phases at old ages and/or very high metallicities; (v) to compare results for the same type of SSPs but different metallicities and enhancement in α -elements; (vi) finally, to mention at least the effect of the enrichment law $\Delta Y/\Delta Z$.

(i) **Relative contribution by different phases.** To this aim the SSPs have been split into five evolutionary phases, i.e. (1) up to the main sequence turn-off (TO), (2) from the TO to the tip of the RGB (T-RGB), (3) from this to the end of core He-burning (HeB), (4) from this stage to the end of the TP-AGB, and finally (5) from this latter down to the formation of Planetary Nebulae and incipient White Dwarf cooling sequence (P-AGB)⁵. We have considered the SSPs by TPD96 *with solar metallicity and no enhancement in α -elements* ($\Gamma=0$). Although these SSPs are somewhat different from the corresponding ones by SGWC00, they offer the advantage that the various evolutionary phases have already been marked by the authors.

In Fig. 6 we show the relative contribution of each phase as function of the SSP age. The relative contribution is defined as follows

$$\left| \frac{\Delta \mathcal{I}_j}{\mathcal{I}^{SSP}} \right| = \left| \frac{\mathcal{I}_j - \mathcal{I}_{j-1}}{\mathcal{I}^{SSP}} \right| \quad (29)$$

where \mathcal{I} stands for the generic index, j for the phase running from 1 to 5 ($j-1=0$ is the main sequence), \mathcal{I}^{SSP} for the total, and finally the phase contribution \mathcal{I}_j is calculated according to eqn. (18).

On the average, lumping together the various steps in three major contributions and neglecting details depending on the particular index under consideration, we find $\Delta \mathcal{I}_{TO}/\Delta \mathcal{I}_{MS}=0.1$, $\Delta \mathcal{I}_{T-RGB}/\Delta \mathcal{I}_{TO}=0.3-0.5$, $\Delta \mathcal{I}_{AGB+P-AGB}/\Delta \mathcal{I}_{T-RGB}=0.1$.

(ii) **Neglecting late evolutionary phases.** Since not all SSPs in literature contain all evolutionary phases predicted by the theory of stellar evolution (in some extreme cases they do not extend beyond the TO or the T-RGB) it is worth looking at the uncertainty introduced in the indices by neglecting late evolutionary phases. To this aim we have calculated the indices of *fictitious* SSPs whose last evolutionary phase is the TO, the T-RGB, the end of core HeB, the end of the TP-AGB, and the P-AGB. Once again, the SSPs in use are those by TPD96. Since no other evolutionary phase is supposed to exist beyond the considered termination stage, the resulting index is physically consistent even though it does not correspond to a real value.

The results of this experiment are shown in Fig. 7 which displays the difference

⁵ To be precise this classification strictly applies to SSPs older than say 0.1 Gyr, i.e. those whose TO mass is smaller than about $5 M_{\odot}$.

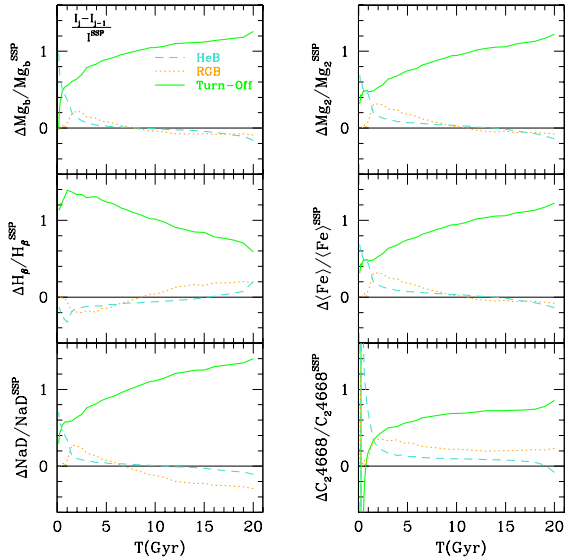


Figure 6. The relative contribution to an index by each phase as function of the age (in Gyr). The SSPs are those by TPD96 with $Z=0.02$ and $\Gamma=0$. The *solid*, *dotted* and *dashed* lines show the contribution from TO, T-RGB, and HeB phases respectively. See the text for more details.

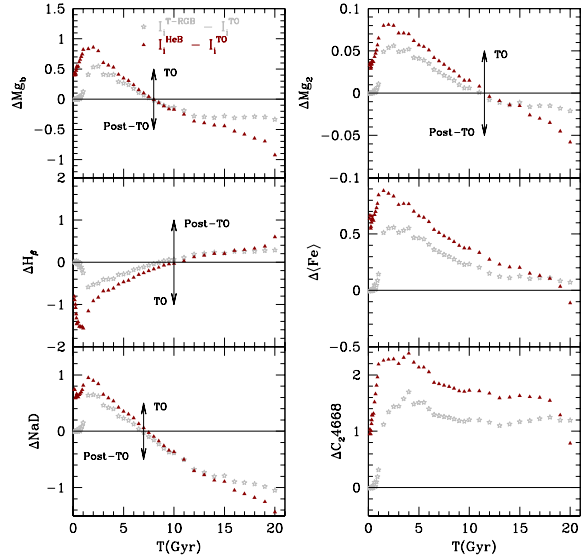


Figure 7. Indices from truncated SSPs, whose last evolutionary stage is the TO, the T-RGB, and the end of the HeB, as function of the age T in Gyr. The displayed quantities are the differences $\Delta I = I^{\text{T-RGB}} - I^{\text{TO}}$ (empty stars) and $\Delta I = I^{\text{HeB}} - I^{\text{TO}}$ (filled circles). The SSPs are those by TPD96 isochrones with $Z=0.02$ and $\Gamma=0$.

$$\Delta I = I^{\text{Phase}} - I^{\text{TO}} \quad (30)$$

For the sake of simplicity we display only the quantities $\Delta I = I^{\text{T-RGB}} - I^{\text{TO}}$ and $\Delta I = I^{\text{HeB}} - I^{\text{TO}}$.

It immediately clarifies what follows: (a) The RGB and

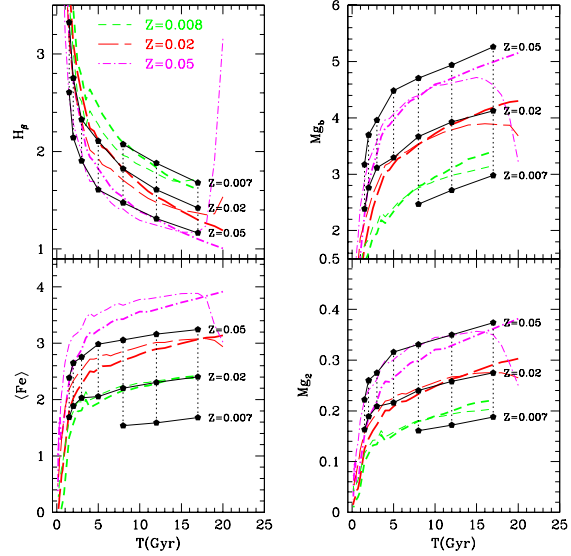


Figure 8. Comparison of four selected indices calculated with different SSPs and abundance patterns. All the indices are plotted as functions of the age in Gyr and for different metallicities as indicated. The thin lines are the indices calculated with the TPD96 SSPs including all evolutionary phases. The thick lines are the same but for SSPs limited to the T-RGB phase. The metallicities are $Z=0.008$, 0.02 , and 0.05 (*dashed*, *long-dashed* and *dot-dashed* respectively). The full circles joined by thin solid and dotted lines are the indices of the Worthey (1994) grid for metallicity $Z=0.007$, 0.02 , and 0.05 as indicated.

HeB stages may significantly affect the total index as already known from the analysis of the relative contributions; (b) Depending on the age and index under examination the Post-TO phases may either increase or decrease the index expected from the sole stars up to the TO. When the difference is positive, neglecting stages beyond the TO and/or the T-RGB means that the index in question is underestimated (often by a significant amount). The opposite when the difference is negative; (c) In any case all phases beyond core HeB do not significantly contribute to the final value of an index.

Chief conclusion of the above analysis is that detailed and accurate calculations of SSPs throughout all evolutionary phases are the main prerequisite to obtain reliable indices. Passing to the SGWC00 library of SSPs, we recover most of the trends presented above, even if there are significant differences in the details.

(iii) **Which of the Padova SSPs get closer to TFWG00?** Going back to the SSPs adopted by TFWG00, they are not strictly equivalent to those in usage here first because they are for solar-scaled compositions and second they stand on stellar models calculated with somewhat older physical input. To cope with the latter point of inconsistency, we prefer to compare the SSPs of Worthey et al. (1994) with the TPD96. It is worth recalling that both libraries (Worthey et al. (1994) and TPD96) even if in a different fashion, include all stellar evolutionary phases.

In Fig. 8 we compare the indices calculated with the TPD96 SSPs including all evolutionary phases (thin lines)

with those obtained by Worthey (1994) (full dots and lines). The two grids of models differ in several important details: (a) There is a large offset in $\langle \text{Fe} \rangle$ at given metallicity; (b) At old ages the indices based on TPD96 tend to reverse their trend. The effect is more pronounced for high metallicities. The reason of this is the anomalous behavior of the core HeB and later phases at increasing metallicity to be discussed below. (c) Remarkably, the Worthey et al. (1994) grid supposedly extending up to the latest evolutionary phases is actually in closer agreement with the TPD96 truncated at the T-RGB. All this could suggest that part of the disagreement could reside in the way the HeB stages are included by Worthey et al. (1994). However, the same argument cannot be invoked for the indices by TMB03, which are based on stellar models/SSPs that are calculated with accuracy comparable to that of the TPD96 models.

(iv) **Effect of core HeB and later phases.** Comparing the complete SSPs of TPD96 with those by SGWC00, see Fig. 2, we note the important effect on the indices caused by core HeB stars at varying age and metallicity. In brief, at normal metallicities, say up to $Z \approx 0.008$, a sort of upper limit for stars in Globular Clusters, at very old ages (older than about 15 Gyr) the indices suddenly increase (H_β) or decrease (e.g. Mg_2 , Mg_b , $\langle \text{Fe} \rangle$). The same occurs for metallicities greater than $Z \approx 0.008$, but the age at which the trend is reversed gets lower and lower at increasing metallicity. The reversal of the indices at old ages and/or high metallicities is fully explained by the behavior of core HeB stars. Limiting the discussion to low mass stars and old ages in turn, the rule is that core HeB (or HB morphology) takes place closer and closer to the Hayashi line at decreasing age and/or increasing metal content. The trend is the result of three concurring effects: the value of the TO mass (age), the amount of mass lost at the T-RGB (details of the adopted mass-loss rate are very important in this context), and the metallicity itself. Under current estimates for the efficiency of mass-loss, the HB phase gets redder and redder at increasing metal content and the AGB phase takes place along the Hayashi line (see Chiosi et al. 1992, for all details). This is the typical behavior of stars in Globular Clusters. However, as pointed out long ago by Brocato et al. (1990), Castellani & Tornambé (1991), Horch et al. (1992), Dorman et al. (1993), Fagotto et al. (1994), and Bressan et al. (1994), if the metallicity happens to be higher than the typical value for the most metal-rich globular clusters, this simple scheme breaks down. In brief at high metallicity (close to the solar value), the evolution does not proceed toward and along the AGB, but toward a slow phase taking place at high effective temperature without going back toward the AGB (the so-called AGB-manqué phase, see Greggio & Renzini 1990, for more details). For solar and twice solar metallicity, the blue phase begins during the shell He-burning. For 3 times solar metallicity it begins during the late stages of core He-burning. For still higher metallicity a large fraction of the core He-burning lifetime is spent at very high effective temperature and high luminosity, see Bressan et al. (1994) for more details. All this would immediately reflect onto the broad-band colors and indices that are sensitive to the flux emitted in UV-visible part of the spectrum. The effect is that many indices reverse their trend at increasing age and increasing metallicity as already shown in Fig. 8 for the indices H_β , Mg_2 , Mg_b , and $\langle \text{Fe} \rangle$. The SSPs by SGWC00 do

not display the above trend (at least in range of ages and metallicities they have considered) because of the different physical input of the stellar models, in particular the mixing length, the opacity, and the prescription for mass-loss during the RGB and AGB phases (see SGWC00 for details).

(v) **Varying metallicity and Γ .** Although this topic has already been addressed in Section 6 and partially shown in Fig. 2, it is worth of interest to stress here once more how the indices, based on the same type of stellar models, depend on Z and Γ considering the whole range of values spanned by the parameters. The SSPs are those by SGWC00. The results are shown in Fig. 9 as function of the age, metallicity, and Γ . The thin lines are the case with $\Gamma=0$, whereas the thick lines are for $\Gamma=0.5$. Of the four indices on display, Mg_2 has the lowest dependence on Γ , the opposite occurs for Mg_b . At increasing Γ , the index $\langle \text{Fe} \rangle$ decreases simply due to the fact that higher values of Γ imply lower values of $[\text{Fe}/\text{H}]$. The dependence on Z at given Γ is as one would expect from simple considerations. A special remark is due to H_β , which at increasing Γ and Z shows an unexpected trend. First of all, it significantly increases passing from $\Gamma=0$ to 0.5. Second, for the case with $\Gamma=0.5$ the dependence on the metallicity is reversed and even more relevant here it is no longer monotonic. At ages older than about 3 Gyr, the more metal-rich SSPs reach the maximum value in the age range 5 to 10 Gyr and then move to lower values. All these trends are in agreement with the entries of Table 5. Similar results are found for the SSPs of TPD96.

(vi) **The enrichment law $\Delta Y/\Delta Z$.** The Padova database of stellar tracks has been calculated assuming a suitable law of chemical enrichment $\Delta Y/\Delta Z$, i.e. the relation $Y - Y_p = \beta(Z - Z_p)$, where Y_p and Z_p are the primordial helium and metal abundances, respectively, and β is the enrichment ratio. If $Z_p=0$ is an obvious choice, excluding the effect of primordial PopIII stars that in principle could alter both Y_p and Z_p (Marigo et al. 2002; Salvaterra & Ferrara 2003), the choice of Y_p and β is more difficult. A recent observational estimate by Peimbert & Peimbert (2002) yields $Y_p=0.23$ and $\beta=2.1 \pm 0.5$. Bertelli et al. (1994) have adopted $Y_p=0.23$ and $\beta=2.5$ (Pagel 1989), whereas SGWC00 have chosen $Y_p=0.23$ and $\beta=2.25$ as in Girardi et al. (2000). Other databases of stellar tracks and SSPs have been calculated and/or assembled either explicitly or implicitly assuming similar enrichment laws, e.g. the SSPs by Worthey (1994) and TFWG00 in turn have $Y_p=0.228$ and $\beta=2.7$, whereas Maraston (1998) adopts $Y_p=0.23$ and $\beta=2.5$ but for extremely high metallicities for which adopts the Salasnich et al. (2000) prescription. In many other cases the $\Delta Y/\Delta Z$ relationship is simply ignored. Unfortunately no useful set of stellar tracks can be found in literature, in which a large range of metallicities are explored at constant Y . Basing on the few and limited set of stellar tracks to disposal, suffice it to note here that stellar models with the same Z and higher Y tends to be brighter and bluer than those of lower Y . This would immediately reflect onto the colors and indices of the associated SSPs. This is a point to keep in mind when exploring the effect of Z because depending on the chosen set of models, varying Z can actually mask also important effects of Y .

Final remark. The above discussion clarifies first that not all stellar models are equivalent – indeed important dif-

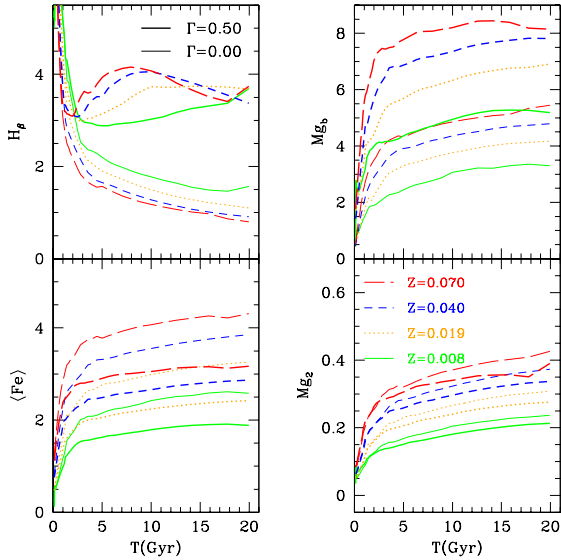


Figure 9. Dependence of the indices H_β , Mg_2 , Mg_b , and $\langle Fe \rangle$ on the age, metallicity and degree of enhancement. The metallicities are $Z=0.008$ (solid lines), 0.019 (dotted-dashed lines), 0.04 (dashed lines), and 0.07 (long dashed lines). The thin lines are for $\Gamma=0$, whereas the thick lines are for $\Gamma=0.5$. The SSPs are those by SGWC00 with the corrections by TB95.

ferences exist even among libraries calculated by the same group, see e.g. TPD96 and SGWC00 (the most relevant differences here are the opacities and the prescription for the mass-loss rate at the T-RGB) –, second that details of stellar models might bear very much on the final correlation between indices and metallicity and age. This latter point is not trivial considering that high metallicity stars (well above solar) could exist in the population mix of EGs, see Bressan et al. (1994). Finally, the effect of Γ is of paramount importance and opposite to what expected from simple-minded considerations.

8.2 Comparison between SGWC00 and TMB03

In view of the discussion below, it is worth of interest to compare the indices calculated by TMB03 with ours derived from the SGWC00 stellar models and set of abundances. This is shown in Fig. 10 for three selected indices, i.e. H_β , Mg_b and $\langle Fe \rangle$, $\Gamma=0, 0.35$ and 0.50 , and several values of the metallicity in common ($Z=0.008, 0.019, 0.04$, and 0.07). For $\Gamma=0$ the two sets of models almost exactly coincide, whereas at increasing Γ they progressively differ especially as far as H_β and Mg_b are concerned. For any value of Z , our indices are higher than those of TMB03. The differences at increasing Γ are likely due to either the adopted enhancement factors for individual elements or the correcting procedure or both. We will come back to this issue in Sects. 9 and 9.6.

8.3 Extrapolating the grids of indices

There is another important point to be made that could bear very much on the final results, i.e. the way grids of

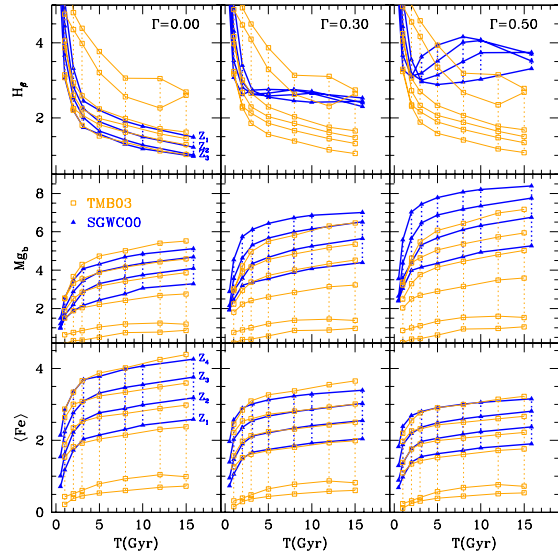


Figure 10. Comparison between the indices calculated with the SGWC00 mixture (thick lines) and those by TMB03 with the TFWG00 mixture (thin lines). The curves are labelled by the metallicity $Z_1=0.008$, $Z_2=0.019$, $Z_3=0.040$, $Z_4=0.07$. The set by TMB03 contains more metallicities of lower value: the top curves in the panels for H_β and the bottom ones in the panels for the remaining indices. While there is coincidence for Mg_b and $\langle Fe \rangle$, at increasing Γ the values of H_β disagree.

stellar models/SSPs/indices are extrapolated from existing tabulations.

To illustrate the point let us have a close look to the extension made by TFWG00 of the Worthey (1994) grid of SSPs already shown in the various panels of Fig. 8. The maximum age of the SSPs is 17 Gyr and three values of metallicity are considered, i.e. $Z=0.007, 0.02, 0.05$. For ages older than about 5 Gyr the behavior of the various indices under examination is very smooth, almost linear in the two parameters. Basing on this, the linear extrapolation of the indices to older ages, higher metallicities, and higher values of Γ seems to be reasonable. Indeed the grids have been extrapolated by TFWG00 to ages up to 30 Gyr and metallicities up to $Z=0.07$.

However we have amply discussed that stellar models, SSPs, and indices in turn are very sensitive to age and metallicity, and that past the T-RGB some unexpected evolutionary phases may appear largely affecting the regular trend of the indices in previous stages, at younger ages and/or lower metallicities. The effect is clear comparing the old SSPs/indices of TPD96 to those of SGWC00 and the experiments on the indices that we have performed with the TPD96 SSPs truncated at different evolutionary phases. Furthermore, we have already noticed that TFWG00 grids of indices even in the age and metallicity ranges covered by the original Worthey (1994) models are much akin to the TPD96 ones truncated at the T-RGB.

Therefore the use of incomplete grids of stellar models and the straight extrapolation of stellar models/indices to much older ages and/or much higher metallicities might not be a safe procedure to adopt.

8.4 Calculating and correcting SSP indices for α -enhancement

To derive the indices of SSPs and correct them for α -enhancement two different procedures are currently in use:

(i) *The star by star case.* This is the method followed by us as described in Section 6: individual stars along an isochrone of given metallicity and Γ are approximated by the elemental bins of small $\Delta \log L/L_{\odot}$, ΔT_{eff} . For each bin the indices are derived from the *Fitting Functions* (which in turn depend on $\log T_{\text{eff}}$, $\log(g)$, and $[\text{Fe}/\text{H}]$). The indices of the elemental bins are corrected for enhancement by means of a suitable technique, and finally the total indices of the SSP are calculated according to relations (15).

(ii) *The phase by phase case.* TMB03 and TFWG00 split the basic SSP model in three evolutionary phases: dwarf (D), turn-off (TO), and giants (G), derive the indices for the each phase summing up the contribution from the elemental isochrone bin, correct the indices of each sub-phase by means of the TB95 *Response Functions* and finally get the total indices of the SSP according to relations (18) in Sect. 4.

To correct the indices for α -enhancement by means of the TP95 *Response Functions* two possible approximations are in literature. They have been already been presented in Sect. 4, i.e. relations (19) and (27).

We will see that passing from method (i) plus relation (19) to method (ii) plus either relation (19) as in TFWG00 or (27) as in TMB03, the indices will not differ by more than 15% provided all other conditions are the same.

9 WHY SUCH BIG DIFFERENCES? THE ABUNDANCE PATTERNS

Another important and obvious source of disagreement are the patterns of abundances especially when α -enhanced mixtures are adopted. As matter of fact, a star index depends on the gravity, T_{eff} (that are function of the gross chemical parameters, Y and Z) and detailed chemical composition at the surface ($[\text{Fe}/\text{H}]$ at least). This is particularly relevant when corrections are applied to pass from solar-scaled to α -enhanced mixtures. In other words, an index is likely to depends more on the detailed pattern of abundances adopted in the *Fitting Functions* and *Response Functions* than on the gross chemical parameters of the underlying stellar models.

Furthermore, comparing the distributions in age, metallicity and Γ (Fig. 4) based on the SGWC00 indices with those by TFWG00 for their C^0O^+ model is not fully correct because the two patterns of abundances are not the same.

To clarify the subject we perform several experiments combining different sets of isochrones with different choices for the abundance patterns, the α -enhanced mixtures in particular.

9.1 Case A: The SGWC00 set of abundances

In this section we remind the reader that a new set of indices has been calculated adopting the isochrones by SGWC00 and the total enhancement $\Gamma=0.50$. Since the abundance pattern of these models has already been presented in Sect. 7.2 no more details are given here. In the following we will refer to the grids of the SGWC00 indices with $\Gamma=0$,

0.35, and 0.50 as Case A (see the range of this grids in Sect. 7.2).

9.2 Case B: The C^0O^+ model of TFWG00

Since the TFWG00 indices are calculated from solar-scaled stellar models-SSPs on the top of which different degrees of enhancement are added by means of the TB95 calibration (to a first approximation the effect of enhancement on stellar models is neglected) we have to recover the same situation. To this aim we adopt the SSPs by TPD96 up to the P-AGB phases (see section 8.1 above), and the pattern of enhanced abundances as in the model by TFWG00 labelled C^0O^+ .

The abundance patterns presented by TFWG00 have three groups of elements:

Enhanced elements⁶ : N, Ne, Na, Mg, Si, S, Ti plus sometimes C and/or O. They are indicated by TFWG00 as E-elements;

Depressed elements⁷ (i.e. Fe-peak Group): Cr, Mn, Ca, Co, Ni, Cu, Zn, Fe, that we denote as D-elements;

Fixed elements, which means solar-scaled.

Furthermore, different values can be assigned to C and O. In their model C^0O^+ , C belongs to the group of fixed elements whereas O to the group of enhanced elements.

To properly compare our results with those by TFWG00, we must establish the correspondence between our definition of Γ with that adopted by TFWG00. According to their notation, our eqn. (4) can be cast in the following way

$$[\text{Fe}/\text{H}] = [\text{Z}/\text{H}] - \mathcal{A}[\text{E}/\text{Fe}]$$

or

$$\Delta[\text{Fe}/\text{H}] = -\mathcal{A}\Delta[\text{E}/\text{Fe}]$$

at fixed $[\text{Z}/\text{H}]$ where “E” refers to the mass fraction of elements that are specifically enhanced and \mathcal{A} is a generic constant of proportionality. This means that $\mathcal{A}[\text{E}/\text{Fe}]$ corresponds to Γ of eqn. (4).

In TFWG00 the enhancement factor is let vary from $[\text{E}/\text{Fe}]=-0.30$ to 0.75 which means that the ratio $[\text{O}/\text{H}]$ increases from -0.021 up to 0.053, whereas $[\text{C}/\text{H}]$ remains equal to 0. It is worth noticing that the case with $[\text{E}/\text{Fe}] = -0.30$ and $[\text{O}/\text{H}]=-0.021$ considered by TFWG00 actually corresponds to a decrease of the α -elements and $[\text{O}/\text{H}]$ with respect to the solar pattern.

In Table 6 (the analog of Table 4 in TFWG00) we summarize the abundance ratios we have adopted to correct the indices according to their model C^0O^+ and our definition of Γ given by eqn. (4) or (12). Column (1) gives the constant \mathcal{A} . Column (2) yields the enhancement factor ($[\text{E}/\text{Fe}]$ or equivalently Γ/\mathcal{A} in our notation). Columns (3) and (4) list the amount of depression and enhancement for E- and D-elements, respectively. Finally columns (5) through (8) give the mass fractions of C, O, Fe and enhanced elements.

⁶ They are scaled up by the same factor. The dependence of the indices on Ti is however not taken into account by TFWG00.

⁷ They are scaled down by the same factor.

Table 6. Element mass fractions in metals for non solar abundance ratios according to the model C^0O^+ of TFWG00.

\mathcal{A}	$\Delta[E/Fe]$	$\Delta[D/H]$	$\Delta[E/H]$	X_C/Z	X_O/Z	X_{Fe}/Z	X_E/Z
0.9288	-0.30	0.28	-0.021	0.174	0.433	0.137	0.252
0.9288	0.00	0.00	0.000	0.174	0.482	0.072	0.265
0.9288	0.32	-0.30	0.023	0.174	0.506	0.036	0.279
0.9288	0.75	-0.70	0.053	0.174	0.508	0.015	0.300

The ranges of age, metallicity and enhancement spanned by our new grid based on the TPD96 SSPs is $0 \leq T \leq 20$ Gyr, $0.008 \leq Z \leq 0.100$ (or $-0.42 \leq [Z/H] \leq 0.92$), and $-0.28 \leq \Gamma \leq 0.70$ (or $-0.30 \leq [E/Fe] \leq 0.75$). The grid⁸ contains four values of metallicity, namely $Z=0.008, 0.02, 0.05$ and 0.1 which correspond to $[Z/H]=-0.42, 0, 0.47$, and 0.92 according to the TFWG00 notation. For each metallicity we have corrected the indices by using eqn. (19) for the different values of Γ given in Table 6. Subsequently, we have interpolated among the four grids in steps of $\Delta\Gamma = \mathcal{A}\Delta[E/Fe] = 0.02$ or equivalently $\Delta[Z/H] = 0.03$. Finally, the age steps are the same of the original isochrones. *These experiments allow us to test the effect of a simple enhancement scheme on the standard stellar models/SSPs.* These models are referred to as Case **B**.

9.3 Case C: The TPD96 isochrones and the SGWC00 mixture

Finally, we consider the case of indices calculated with the old SSPs of TPD96 and the mixtures of chemical abundances of SGWC00, i.e. $\Gamma=0, 0.35$, and 0.50 . The grids⁹ span the ranges $0 \leq T \leq 20$ Gyr, $0.008 \leq Z \leq 0.100$ (or $-0.42 \leq [Z/H] \leq 0.92$), and $0.00 \leq \Gamma \leq 0.50$. *This case allows us to test the effect of a complex abundance scheme on standard SSPs.* Models of this type are referred to as Case **C**.

9.4 Comparing the indices of Cases A, B and C

In this section we quickly compare the results for the three cases above. In Fig. 11 we present the six indices under consideration as function of the age for the case with solar composition ($Z=0.019$) and enhancement $[E/Fe]=0.31$ (we adopt here the notation by TFWG00). It is soon evident that Cases **A** and **C**, whose indices are calculated with same pattern of abundances, yield nearly the same results despite the fact that they stand on different SSPs/isochrones. The largest difference is with Case **B** which has a different set of abundances. This experiment clearly shows that the abundance ratios are the key parameter. The opposite conclusion reached by TFWG00 is likely due to an insufficient exploration of the parameter space since they limit the analysis to varying only C and O. We show in Section 9.6 how the adoption of a particular set of abundance ratios would reflect onto the age estimate.

⁸ We adopt $Z_\odot=0.020$ and $X_\odot=0.700$ to replace Z with $[Z/H]$, and the constant $\mathcal{A}=0.9288$ to convert Γ into $[E/Fe]$.

⁹ We adopt $Z_\odot=0.02$ and $X_\odot=0.700$ to replace Z with $[Z/H]$.

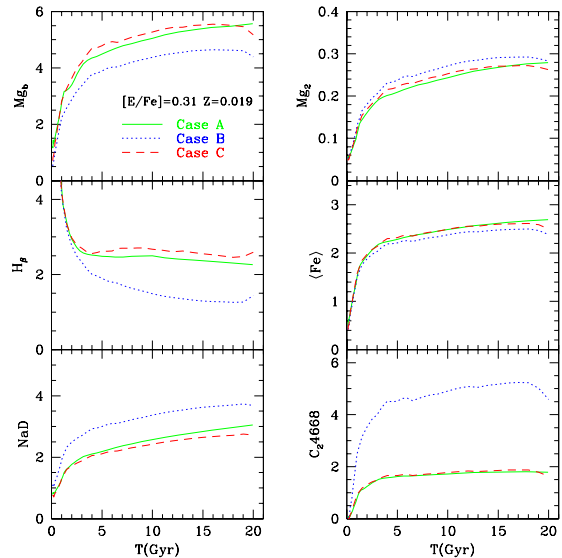


Figure 11. Evolution of six indices (Mg_b , Mg_2 , H_β , $\langle Fe \rangle$, NaD and C_{24668}) as function of the age according to the recipes of Cases **A** (solid lines), **B** (dotted lines), and **C** (long dashed lines) and limited to the solar metallicity $Z=0.019$.

9.5 Ages, metallicities and Γ s from Cases A, B and C

The results obtained from the *Minimum-Distance Method* applied to the González's sample and the different sets of theoretical indices are summarized in Fig. 12. Uncomfortably, each case yields different results due to the different assumption for the input SSPs and pattern of abundances. Looking at the cases in more detail, we note the following:

(i) Case **A** – Ages clusters in two groups, from 1 to 15 Gyr, and 19 to 20 Gyr, where the majority of the population is found. The metallicity now goes from $[Z/H] = -0.1$ to 0.2 with a tail to higher values. On the average it is lower than in TFWG00. The enhancement factor peaks at $\mathcal{A}[E/Fe]=0.1-0.2$ being about 0.1 dex lower than in TFWG00.

(ii) Case **B** – The age distribution is much similar to that of TFWG00. The only minor difference is the concentration of objects in the age range 3 to 5 Gyr (about 45% of the galaxies fall in this age bin). The metallicity peaks at about $[Z/H]=0.5$, and $\mathcal{A}[E/Fe]=0.2-0.4$. In TFWG00, the ages almost evenly distribute from 1 to 16 Gyr with very few objects of 20 Gyr, the metallicity is centered at $[Z/H]=0.2$ with tails on both sides, i.e. a factor of two lower, the enhancement factor peaks at $\mathcal{A}[E/Fe]=0.2$, a factor 1.5 lower.

(iii) Case **C** – The age distribution is much similar to that of Case **A**, even though the maximum age is now shifted

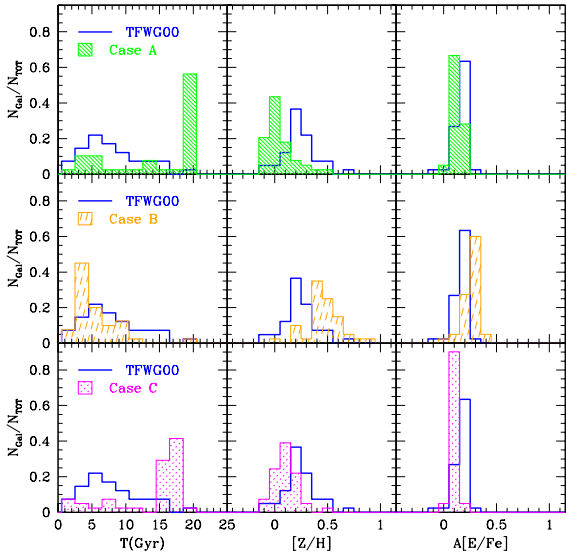


Figure 12. Summary of the results for Cases **A**, **B** and **C**. The top three panels show the age (in Gyr), metallicity ($[Z/H]$) and enhancement ($A[E/Fe]$) distributions, from left to right for Case **A** models. The thick lines are the TFWG00 solution, drawn here for comparison. The mid three panels are the same but for Case **B** models. Finally the bottom three panels are the results for Case **C** models.

to the range 15-18 Gyr. The distribution in metallicity is nearly the same as in TFWG00, only 0.1 dex lower, whereas the enhancement factor peaks at $A[E/Fe]=0.1$ where the majority of galaxies are found with a short tail extending down to $A[E/Fe]=0$.

Comparing Case **B** to Case **C** the effect of different patterns of chemical abundances in the α -enhanced mix is revealed, whereas comparing Case **A** to Case **C**, the effect of different stellar models/isochrones is highlighted. It is soon evident that the pattern of abundances in the enhanced mix plays the dominant role. The results of TFWG00 and TMB03 are indeed recovered when the abundance pattern is the same, this almost independently of the SSPs in use.

9.6 The nasty Titanium

The lengthy and detailed discussions of the various aspects of the problem carried out in Sects. 8 and 9 have highlighted that the abundance pattern for the α -enhanced mixtures is the key parameter. However, pinning down the factor truly responsible of the disagreement between our study and the previous ones has so far eluded our efforts.

There is only one aspect of the whole problem, which has not yet been analyzed, i.e. the detailed comparison element by element for which variations with respect to the solar mix are adopted.

As already mentioned, at fixed total metallicity SGWC00 adopt a mixture in which O, Ne, Mg, Si, Ca, Ti, and Ni are enhanced by different factors with respect to the Sun. All other elements in their list, specifically C, N, Na, Cr and Fe keep the solar abundance relative to Fe.

TFWG00 let the abundance of N, Ne, Mg, Na, Si, S

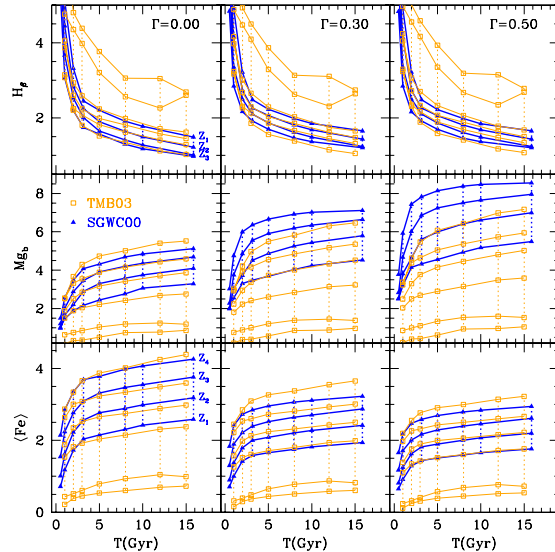


Figure 13. Comparison of the indices for SSPs with solar metallicity, $\Gamma=0.3$ and 0.5 , and $[Ti/Fe]=0$, calculated by TMB03 (thin lines) and by us. The curves are labelled by the metallicity, i.e. $Z_1=0.008$, $Z_2=0.019$, $Z_3=0.040$, $Z_4=0.07$. For the metallicities in common, the coincidence is remarkably good.

to increase, that of C and O either to increase or to remain constant, that of Fe, Ca, Cr to decrease, and that of all other elements to remain constant. However, they have ignored the dependence of the line strength on Ti as “TB95 make contradictory statements about its inclusion in their model atmospheres” (see the footnote n. 5 in TFWG00). The mixture adopted by TMB03 is the same of Model 1 by TFWG00, but they include Ca and Ti in the group of enhanced elements.

Looking at the *Response Functions* of TB95, those of Mg, and Ti are the dominants ones in particular for the Cool Dwarfs. For an enhancement factor 0.3, the TFWG00 and TMB03 mixtures imply $[Mg/H]=0.023$ and $[Ti/H]=0.023$. Both are significantly smaller than our values listed in Table 2, the one for Ti in particular which is a factor of ten smaller. We expect therefore that differences in the degree of enhancement adopted for these elements should bear very much on the final results. To check this point we have systematically changed the quantities $[X_{el}/Fe]$ and derived the relative variations $\Delta I/I$ for the Cool-Dwarf, Cool-Giant, and Turn-Off stars of TB95. As expected Mg and Ti have a large impact, whereas all remaining elements do not play a significant role. Since Mg is always enhanced by a comparable factor in all studies under examination, whereas Ti is strongly enhanced only in SGWC00, we suspect that the ultimate cause of the disagreement between TFWG00, TMB03 and the present study is the degree of enhancement assumed for this element. Table 7 summarizes the results of the analysis. The overabundance factor $[Ti/Fe]$ is increased in steps of 0.2 dex from $[Ti/Fe]=0$ to the value adopted by SGWC00 for $\Gamma=0.35$, i.e. $[Ti/Fe]=0.63$, and to the value $[Ti/Fe]=0.87$ derived by us for $\Gamma=0.50$. Limited to the case of SSPs with $Z=0.019$ (similar results are found for other metallicities), the fractional variations $\Delta I/I$ and indices are calculated.

Table 7. Effects of changing the enhancement factor [Ti/Fe] of Titanium: Fractional variations $\Delta I/I$ and Indices.

$\Gamma = 0.35$					$\Gamma = 0.50$				
[Ti/Fe]	Index	CD	CG	TO	[Ti/Fe]	Index	CD	CG	TO
0.00	H $_{\beta}$	0.020	-	-0.003	0.00	H $_{\beta}$	-0.041	-	-0.007
	Mg $_b$	0.144	0.868	0.554		Mg $_b$	0.199	1.440	0.863
	Fe52	-0.166	-0.230	-0.201		Fe52	-0.232	-0.314	-0.294
	Fe53	-0.240	-0.138	-0.344		Fe53	-0.326	-0.193	-0.463
0.23	H $_{\beta}$	0.802	-	0.005	0.27	H $_{\beta}$	0.869	-	0.003
	Mg $_b$	0.155	0.878	0.465		Mg $_b$	0.213	1.453	0.739
	Fe52	-0.155	-0.222	-0.162		Fe52	-0.219	-0.306	-0.253
	Fe53	-0.221	-0.128	-0.316		Fe53	-0.307	-0.182	-0.436
0.43	H $_{\beta}$	1.954	-	0.013	0.47	H $_{\beta}$	2.065	-	0.011
	Mg $_b$	0.165	0.885	0.392		Mg $_b$	0.223	1.464	0.653
	Fe52	-0.145	-0.216	-0.126		Fe52	-0.210	-0.300	-0.221
	Fe53	-0.205	-0.119	-0.291		Fe53	-0.292	-0.174	-0.415
0.63	H $_{\beta}$	3.844	-	0.021	0.67	H $_{\beta}$	4.025	-	0.019
	Mg $_b$	0.175	0.893	0.323		Mg $_b$	0.233	1.474	0.570
	Fe52	-0.135	-0.210	-0.089		Fe52	-0.201	-0.295	-0.188
	Fe53	-0.188	-0.110	-0.265		Fe53	-0.277	-0.165	-0.393
					0.87	H $_{\beta}$	7.239	0.000	0.026
				Mg $_b$		0.244	1.485	0.492	
				Fe52		-0.192	-0.289	-0.154	
				Fe53		-0.261	-0.157	-0.371	

[Ti/Fe]	Log(T)	H $_{\beta}$	Mg $_b$	Fe52	Fe53	[Ti/Fe]	Log(T)	H $_{\beta}$	Mg $_b$	Fe52	Fe53
0.00	9.00	4.438	2.812	1.381	1.139	0.00	9.00	4.425	3.507	1.229	1.011
	9.70	1.898	5.322	2.295	2.067		9.70	1.881	6.558	2.055	1.860
	10.00	1.499	5.791	2.489	2.235		10.00	1.477	7.021	2.239	2.011
	10.15	1.286	6.057	2.617	2.353		10.15	1.264	7.282	2.360	2.118
0.23	9.00	4.493	2.750	1.421	1.166	0.27	9.00	4.488	3.421	1.270	1.039
	9.70	2.065	5.243	2.346	2.110		9.70	2.077	6.448	2.108	1.905
	10.00	1.753	5.723	2.539	2.283		10.00	1.773	6.925	2.291	2.060
	10.15	1.552	6.003	2.665	2.403		10.15	1.573	7.206	2.411	2.170
0.47	9.00	4.554	2.700	1.456	1.191	0.47	9.00	4.551	3.362	1.302	1.061
	9.70	2.306	5.180	2.391	2.150		9.70	2.326	6.373	2.148	1.939
	10.00	2.125	5.669	2.583	2.325		10.00	2.159	6.860	2.331	2.097
	10.15	1.941	5.961	2.709	2.447		10.15	1.976	7.155	2.450	2.209
0.63	9.00	4.639	2.653	1.493	1.217	0.67	9.00	4.638	3.307	1.335	1.082
	9.50	2.709	4.582	2.263	2.027		9.70	2.729	6.303	2.190	1.974
	10.00	2.731	5.618	2.629	2.369		10.00	2.787	6.800	2.372	2.135
	10.15	2.576	5.922	2.753	2.492		10.15	2.635	7.108	2.490	2.249
						0.87	9.00	4.762	3.255	1.369	1.105
					9.70		3.385	6.238	2.233	2.010	
					10.00		3.813	6.745	2.414	2.174	
					10.15		3.712	7.065	2.531	2.289	

While the variations for indices like Mg $_b$, Fe5270, Fe5335 are nearly independent of [Ti/Fe], $\Delta H_{\beta}/H_{\beta}$ greatly increases passing from [Ti/Fe]=0 to higher and higher values. This immediately reflects onto the value of H $_{\beta}$ which follows the same trend in particular for ages older than 1 Gyr. *Is the overabundance of Ti the sole cause of the disagreement between TFWG00, TMB03 and SGWC00?*

To answer this question, we have calculated a new grid of SSPs for which we assume that [Ti/Fe]=0 in the SGWC00 mix and also in our case with $\Gamma=0.50$. We compare the time variation of a few selected indices with those by TMB03. The results are shown in Fig. 13. The agreement is now remarkably good. There is a marginal difference at old ages amounting to the maximum value of 15%, which, as already mentioned, is caused by the correcting procedure, i.e. the star by star versus the phase by phase technique, and the use of relation (19) instead of relation (27).

It easy to foresee that the age, metallicity, and enhance-

ment histograms will not differ too much from those already presented by TFWG00 and TMB03. Since the exercise is trivial we will not go into any detail. Suffice to show in the top panels of Fig. 14 the results we get for the González (1993) sample. No further comments are required here.

The reason for the very old ages we have found for most galaxies using the SGWC00 indices are the much higher values and the non-monotonic age-dependence of H $_{\beta}$ (which usually decreases at increasing age) for α -enhanced indices, which in turn are due to the adopted high values of [Ti/Fe]. The other indices in use are scarcely affected by [Ti/Fe] and always keep a monotonic age dependence. Since most observational H $_{\beta}$ fall in the range 1 to 2, rarely up to 2.5, in a theoretical parameter space favoring high H $_{\beta}$ s, while leaving unchanged the remaining indices, the observational triplet of indices is rendered by pushing the solution (in particular for the age) toward the old age edge of the grid looking for

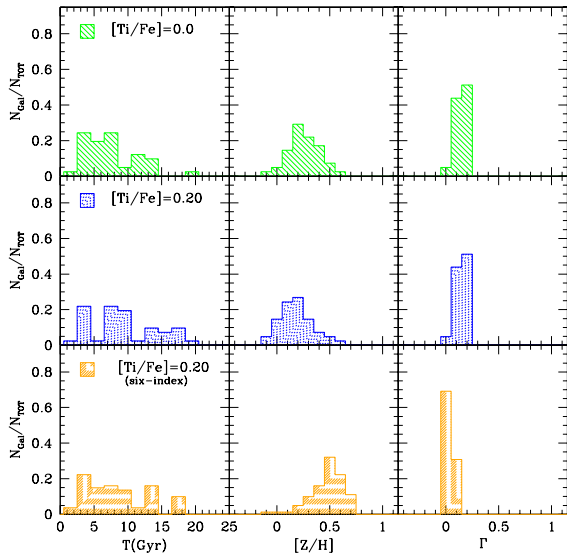


Figure 14. Top Panels: Solutions for models with $[\text{Ti}/\text{Fe}]=0$. The list of enhanced elements is the same as in SGWC00 and Case A models, but for Ti, for which the solar value is adopted. But for one exception all galaxies are younger than 15 Gyr. The results refer to the González (1993) galaxies. The solution is essentially the same as in TFWG00 and TMB03. **Middle Panels:** Solutions for Case D models with $[\text{Ti}/\text{Fe}]=0.20$. Even with the small enhancement factor of Globular Clusters, the solution tend to go back to the starting case presented in Fig. 4. The distributions refer to the same galaxies as in the Top Panels. **Bottom Panels:** Solutions from Case D models with $[\text{Ti}/\text{Fe}]=0.20$ but using six indices instead of three. Now the distributions are for the Trager (1997) catalog.

low H_{β} s. Indeed the most common solution is “very old ages, solar metallicity, and weak enhancement” (see Fig. 4).

9.7 What can we do?

Given the extreme sensitivity of the results to the enhancement factors, the one for Ti in particular, it is worth comparing the choice made by SGWC00 with the most recent determinations obtained by Gratton et al. (2003) for field stars with accurate parallaxes. The mean enhancement for all elements lumped together estimated by Gratton et al. (2003) is $[\alpha/\text{Fe}] \simeq 0.30$ (i.e. $\Gamma=0.30$ in our notation), which roughly corresponds to the case $\Gamma=0.35$ in SGWC00. The enhancement factors for the two sources of data are listed in Table 8. The ratios $[\text{X}_{\text{el}}/\text{Fe}]$ for O, Mg, Si, Ni, Na, Cr, and Fe are almost coincident; that of Ca differs by 0.24 dex, nothing can be said for Ne and S because they are not included in the Gratton et al. (2003) list; finally there is large difference for Ti, which is $[\text{Ti}/\text{Fe}]=0.20$ in Gratton et al. (2003) and 0.63 in SGWC00. Although there is no compelling evidence that the data for Galactic field stars hold good also for elliptical galaxies, for which the enhancement factors could be different (likely higher), we may take the estimate of Gratton et al. (2003) for $[\text{Ti}/\text{Fe}]$ as an indicative value for $\Gamma=0.3$ and use it to predict the abundances for $\Gamma=0.5$. Therefore, we replace $[\text{Ti}/\text{Fe}]$ of SGWC00 with this value, keep unchanged the enhancement factor for the

other species in the list, rescale the abundances as appropriate, and calculate a new grid of indices therein after referred to as Case D. Repeating the analysis for the age, metallicity and enhancement, we get the results presented in the middle panels of Fig. 14. Although the situation is not the same as in Fig. 4, it is also somewhat different from the one presented in the top panel of Fig. 14 because a significant fraction of galaxies with ages from 15 to 18 Gyr are found. This once more confirms the sensitivity of the results to the adopted $[\text{Ti}/\text{Fe}]$. Lower values for this parameter are likely more appropriate. In spite of this, Case D indices will used throughout the second part of this study.

10 IS THE SOLUTION UNIQUE?

Another important question to be addressed is whether different indices yield the same answer as far as age, metallicity and enhancement factor are concerned. In so far we have analyzed the triplet H_{β} , $\langle\text{Fe}\rangle$ and Mg_b because tighten to the González sample. However, several equally representative catalogs of galactic indices are available in literature, for instance the Trager “*IDS Pristine*” sample (Trager 1997), which allow us to derive the above parameters first for a larger number of galaxies and even more relevant here for different groups of indices. In the following we will consider six different indices (Mg_b , Mg_2 , H_{β} , $\langle\text{Fe}\rangle$, NaD and C_24668) and all possible combinations in groups of three. The inclusion of NaD and C_24668 deserves some cautionary remarks. According to Thomas et al. (2003a) both indices are not well calibrated. In addition to this, C_24668 is very sensitive to the C abundance (TB95) and NaD is contaminated by interstellar absorption (Maraston et al. 2003). The only advantage with these indices is their sensitivity to Z and Γ (see the entries of Table 5). Keeping these caveats in mind, we decided to make use of these indices, C_24668 in particular, because looking at the quality ranking we are going to present, the situation is not as bad as it may seem. The observational values are indeed well reproduced by their theoretical counterparts.

An index is considered to be eligible for this kind of analysis if its observational and theoretical value coincide within an uncertainty of 10%. In Table 9 we summarize the results of the ranking analysis for the Case D indices, where Y means that a good correlation between the observational and the theoretically recovered value is found, whereas N is the opposite. Three triplets fully pass the ranking text, i.e. H_{β} - Mg_b - Mg_2 , H_{β} - Mg_b - C_24668 , and Mg_b -NaD- C_24668

The analysis is made for all the galaxies of the Trager (1997) catalog using the *Minimum-Distance Method*. The results for the distribution of age, metallicity and enhancement factor are displayed in the various panels of Fig. 15. Each galaxy is identified by its list number in the Trager (1997) catalog. In each panel we show the range (the vertical bar) spanned by the determinations and their mean value (the full circle) obtained from the different triplets of indices. The top, mid and bottom panels show the age, the metallicity, and the enhancement factor, respectively. It is soon evident that a large spread exists for the same parameter derived from different triplets of indices.

Is the dispersion real? In the sense that each combination of indices is more sensitive to some specific property of

Table 8. Overabundances in SGWC00 and Gratton et al. (2003).

$[X_{el}/Fe]$	α	O	Ne	Mg	Si	S	Ca	Ti	Ni	C	N	Na	Cr	Fe
SGWC00	0.35	0.50	0.29	0.40	0.30	0.33	0.50	0.63	0.02	0.00	0.00	0.00	0.00	0.00
Gratton et al.	0.30	0.51	-	0.39	0.25	-	0.26	0.20	-0.03	0.00	0.00	0.02	-0.02	0.00

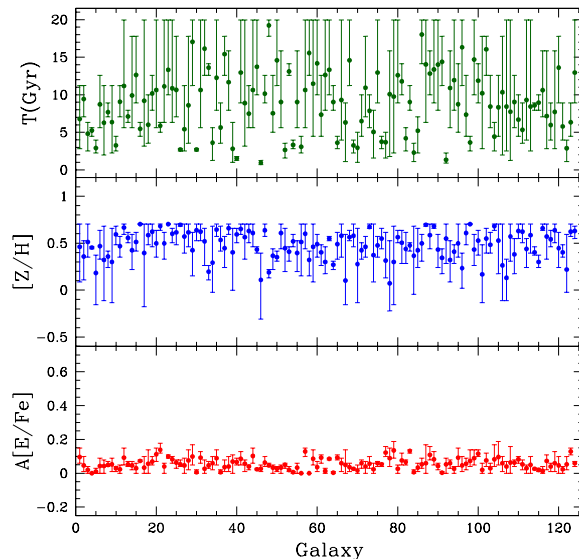
Table 9. Ranking analysis of the index-triplets for Case **D** models.

Index-Triplet	Case D	Index-Triplet	Case D
H_β $\langle Fe \rangle$ Mg_b	N Y Y	$\langle Fe \rangle$ Mg_b Mg_2	Y Y N
H_β $\langle Fe \rangle$ Mg_2	N Y N	$\langle Fe \rangle$ Mg_b NaD	N Y Y
H_β $\langle Fe \rangle$ NaD	N N N	$\langle Fe \rangle$ Mg_b C ₂ 4668	N Y Y
H_β $\langle Fe \rangle$ C ₂ 4668	N N Y	$\langle Fe \rangle$ Mg_2 NaD	N N Y
H_β Mg_b Mg_2	Y Y Y	$\langle Fe \rangle$ Mg_2 C ₂ 4668	N N Y
H_β Mg_b NaD	N Y Y	$\langle Fe \rangle$ NaD C ₂ 4668	N Y Y
H_β Mg_b C ₂ 4668	Y Y Y	Mg_b Mg_2 NaD	Y N Y
H_β Mg_2 NaD	N N Y	Mg_b Mg_2 C ₂ 4668	Y N Y
H_β Mg_2 C ₂ 4668	Y N Y	Mg_b NaD C ₂ 4668	Y Y Y
H_β NaD C ₂ 4668	N N Y	Mg_2 NaD C ₂ 4668	N Y Y

the underlying stellar mix and therefore it traces the stellar component most contributing to the indices in question. Or despite the merit parameter not all triplets are actually good indicators?

We have performed many numerical experiments using fictitious SSPs whose terminal stage is the TO, the T-RGB, and the P-AGB in order to understand if the above dispersion is caused by a different response of triplets of indices to some specific evolutionary phase or group of stars. They are not shown here for the sake of brevity. Even if some indices seem to be weakly sensitive to some particular evolutionary phases, the large differences in age, metallicity and enhancement factor that are always found at varying the triplet of indices in use simply reflect that the solution is not firmly established. This is point of embarrassment because there are no strong arguments to prefer one triplet with respect to others. The dispersion we find means that the solution is not firmly constrained.

To cope with this point of difficulty a last attempt is made using all the six indices at once applied to Case **D** models. The results are shown in the bottom panels panel of Fig. 14. Compared to the results for the same models obtained from the three indices H_β , Mg_b , and $\langle Fe \rangle$ (middle panels), the number of galaxies of very old age has decreased in favor of those with young age (more 90% of the total); the metallicity is on the average 0.3 dex higher, and Γ goes from zero to about 0.1.

**Figure 15.** Age, metallicity, and enhancement factor obtained from the Case **D** models but using different index-triplets, i.e. H_β - Mg_b - Mg_2 , H_β - Mg_b -C₂4668, and Mg_b -NaD-C₂4668. The full circles show the mean value of age, metallicity and enhancement factor estimated for each galaxy of the Trager “*IDS Pristine*” sample whereas the vertical bars indicate the maximum and minimum values. Different triplets yield different results for most galaxies.

11 A FEW REMARKS ON THE TWO INDICES DIAGNOSTIC

The two-indices planes are customarily used to interpret the observational data of galaxies and star clusters. Popular planes are the H_β or $H_{\gamma F}$ vs. $\langle Fe \rangle$ or $[MgFe]$ or Mg_b to derive the age and mean metallicity (Bressan et al. 1996; González 1993; Trager et al. 2000b), and the $\langle Fe \rangle$ vs. Mg_2 to assess the degree of enhancement (Worthey 1992; González 1993; Weiss et al. 1995). The two-indices diagnostics suffers the same uncertainty encountered with the *Minimum-Distance Method*, however at a lower level of complexity because some of the parameters are hidden.

In the following we will examine three typical planes which associate indices that are more sensitive (or insensitive) to some specific parameter. For instance $[MgFe]$ and $[MgFe]'$ do not depend on Γ , the index C₂4668 is very sensitive to Z , partially to Γ and age, and so forth.

In Fig. 16 we show the planes Mg_b vs. $[MgFe]'$ (left panel) and Mg_b vs. C₂4668 (right panel). In each panel are displayed the indices for two values of Γ (0 and 0.35), three values of $[Ti/Fe]$, i.e. 0, 0.20 and 0.63 (filled triangles, empty and filled circles, respectively), and four values of the age, i.e. 16, 8, 3 and 2 Gyr. In Fig. 17 we do the same but for the plane H_β vs. $[MgFe]'$.

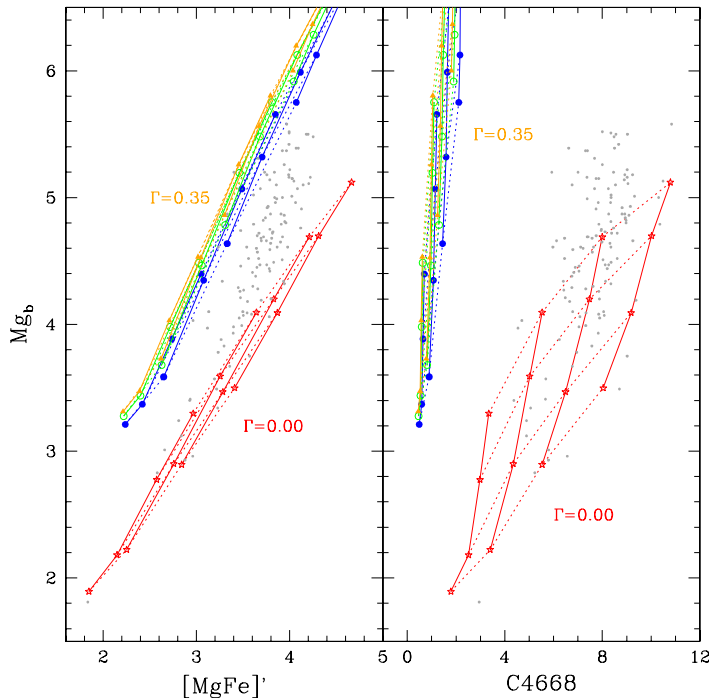


Figure 16. Left Panel: The $[MgFe]'$ vs. Mg_b plane for $\Gamma=0$ and $\Gamma=0.35$ as indicated. In each group four metallicities are shown, i.e. $Z=0.008, 0.019, 0.04, 0.07$ (from left to right). For each Γ and metallicity, we show the results for $[Ti/Fe]=0$ (filled triangles), $[Ti/Fe]=0.20$ (empty circles), and $[Ti/Fe]=0.63$ (filled circles). The dashed lines are the loci of equal age. The theoretical indices on display are those of Case D. The small dots are the data for the Trager “IDS Pristine” sample. **Right Panel:** The same but for the Mg_b vs. C_{24668} plane.

(i) *The Mg_b vs. $[MgFe]'$ plane:* this relationship strongly depends on Γ via the index Mg_b whereas there is little resolving power at varying Z , $[Ti/Fe]$ (see the entries of Table 7) and age. The total enhancement factor of the Trager galaxies goes from $\Gamma=0$ to 0.35 with mean value $\Gamma=0.10$. Nothing can be said for the remaining parameters.

(ii) *The Mg_b vs. C_{24668} plane:* this relationship strongly depends on the metallicity and age for $\Gamma=0$ (solar) whereas it gets worst (little resolving power) for $\Gamma=0.35$. The data cluster in the metallicity range $0.02 \leq Z \leq 0.04$ (with a few exceptions on both sides), are likely compatible with $\langle \Gamma \rangle = 0.10$ (values of Γ as high as 0.35 are likely to be excluded), and seem to span a wide range of ages. Incidentally, the low values of Γ agree with the estimates from the *Minimum-Distance Method* whereas the metallicity is about 0.2 dex lower (see Figs. 14 and 15).

(iii) *The H_β vs. $[MgFe]'$ plane:* this is the most interesting and complex plane to look at. In this plane we have plotted the relationships at varying metallicity, Γ , $[Ti/Fe]$, and age. Each hatched area is enclosed between the two SSPs with the lowest and highest metallicity in our sample, i.e. $Z=0.008$ (left) and 0.07 (right). Along each SSP four values of the age are marked, so that the lines of constant age can be drawn (they are not shown in here for the sake of clarity). The different hatched areas correspond to different combinations of Γ and $[Ti/Fe]$. Starting from the solar case ($\Gamma=0$ and $[Ti/Fe]=0$) we plot the cases $\Gamma=0.35$ and $[Ti/Fe]=0, 0.20$, and $\Gamma=0.35$ and 0.63. The case $\Gamma=0.50$ is of little interest here. Finally, the filled squares are the data.

We emphasize here that other elements like Ti could play the same role: the only requirement is that they have positive fractional variations ($\Delta I/I$) to increasing Γ and $[X_{el}/Fe]$. Assigning age, metallicity and degree of enhancement to a galaxy is a cumbersome affair, because all the three parameters together with possible differences in the abundance ratios $[X_{el}/Fe]$ of some elements concur to scatter the data across this plane. In other words, a galaxy of given H_β and $[MgFe]'$ could have a certain age and a certain metallicity in absence of enhancement, be older and less metal-rich in presence of enhancement, however in this latter case the true age and metallicity depending also on the abundance ratios $[X_{el}/Fe]$ of some elements (the case being represented here by the effect of $[Ti/Fe]$). In addition, the large spread along the H_β axis, which is customarily interpreted as an age spread, could be due to a spread in chemical abundances and abundance ratios. Not necessarily, a galaxy with strong H_β is a young object, The situation becomes very embarrassing and interesting at the same time because another dimension is added to the problem: the spread in H_β could be the signature of different star formation histories and chemical enrichment in turn from galaxy to galaxy. Owing to its implications the issue has been the subject of a companion paper by (Tantalo & Chiosi 2004b).

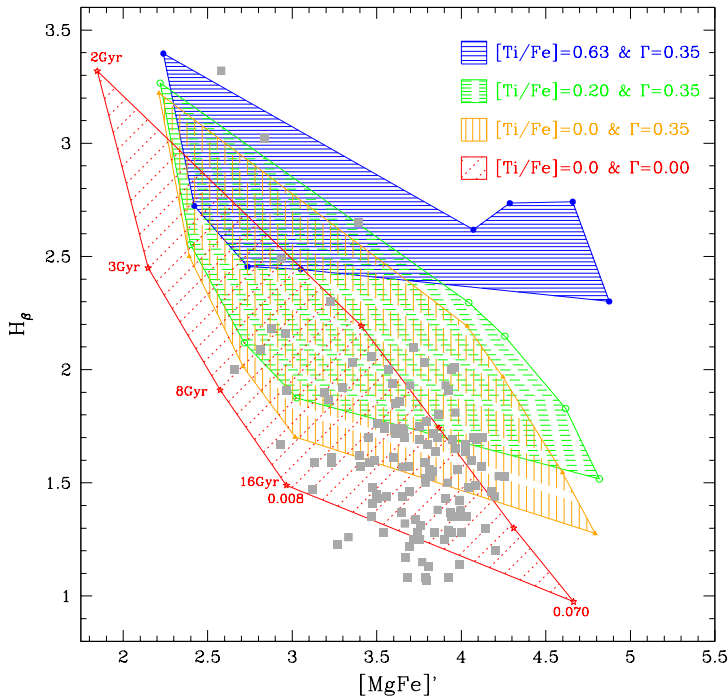


Figure 17. The H_β vs. $[MgFe]'$ plane for different combinations of $\Gamma=0$, metallicity, and $[Ti/Fe]$ as indicated. Each hatched area is enclosed between the two SSPs with the lowest and highest metallicity in our sample, i.e. $Z=0.008$ (left) and 0.07 (right). Along each SSP four values of the age are marked so that the lines of constant age can be drawn (they are not shown in here for the sake of clarity but for the cases of 2 and 16 Gyr). The different hatched areas correspond to different combinations of Γ and $[Ti/Fe]$. The theoretical indices on display are those of Case **D**. The large filled squares are the data from the Trager “*IDS Pristine*” sample.

12 SUMMARY AND CONCLUDING REMARKS

In this study we have investigated the ability of absorption line indices to assess the metallicity Z , the iron content $[Fe/H]$ and Γ in turn, and the age of elliptical galaxies. The analysis has been developed through several steps:

(i) Firstly, we have generated grids of indices based on the SSPs by SGWC00 calculated with chemical composition and opacities enhanced in α -elements, and transformations in which the same chemical mixtures have been adopted. The SSPs and associated indices are for three degrees of total enhancement, i.e. $\Gamma=0, 0.35$, and 0.50 .

(ii) Secondly, we have assessed the response of the indices to variations of age, metallicity, and Γ and found that most of the indices have similar response to three parameters but for a few of them which are definitely more sensitive to metallicity and enhancement. It is worth calling attention that most indices are evenly and weakly depending on the age over large ranges. This is the most crucial aspect of the problem.

(iii) Applying the new grids of SSPs/indices to the popular sample of EGs by González (1993) we have found distributions of age, metallicity and enhancement factors that were too different with respect to previous studies (e.g. TFWG00 and TMB03) of the same data to be simply explained in a simple fashion. This spurred a systematic analysis of the whole problem, in which we have examined the effect of the stellar models and SSPs in use, of the contribution

to the integrated indices of SSPs by stars in different evolutionary phases (TO, T-RGB, HeB, TP-AGB, and later), of the evolutionary behavior of stars with unusual metallicity, the enrichment law $\Delta Y/\Delta Z$, of technical details such as the extrapolation of existing grids of theoretical indices to ages, metallicities, enhancement factors not covered by the original models. Even if each of them bears on the final results. Lastly, we have examined the effect of the particular set of abundance ratios $[X_{el}/Fe]$ that is adopted to reach a certain degree of total enhancement (Γ) at fixed metallicity Z .

(iv) This poses another crucial question because the results much depend on the specific way in which the abundance pattern is built up at given Γ and Z . We have clarified that main reason for the difference between the results obtained with the SGWC00 models and those by TFWG00 and TMB03 is the different assumption made for the ratio $[Ti/Fe]$. The difference originates from the high *Response Function* for this element. We suspect that other elements with high *Response Function* would yield similar effects. This finding adds other dimensions to the problem because the assignment for age, metallicity and Γ much depend on the ratios $[X_{el}/Fe]$ at least from important elements like Mg, Ti, and likely others. The argument is somewhat circular and cannot be easily solved, unless we have additional information on the relative abundances of the enhanced elements.

(v) What we learn from this systematic analysis is that the solution is highly model dependent. The results by TFWG00 and TMB03 can be recovered only if the same pattern of abundances for the enhanced elements is adopted,

i.e. $[\text{Ti}/\text{Fe}] \sim 0$ in particular. Passing to SSPs with $[\text{Ti}/\text{Fe}] > 0$ the tendency is to populate the old age bins of the age distribution. We have taken as upper limit to the abundance ratios $[\text{X}_{\text{el}}/\text{Fe}]$ for some crucial elements like Mg and Ti the values observed in Galactic Globular Clusters.

(vi) In addition to this, we have addressed the question whether the solution found for age metallicity, and enhancement factor is independent of the triplet of indices one has been using. The answer is of course no, in the sense that different triplets having a different resolving power leads to different results. Part of the difficulty resides in the *Minimum-Distance Method* itself which turns out to be inadequate to handle situations in which small variations in the observational and/or theoretical indices imply large variations in the age, metallicity and degree of enhancement. To cope with this difficulty we tried to estimate ages, metallicities, and enhancement in α -elements by simultaneously fitting many indices (six in our case). Though the situation gets better, it is not fully satisfactory.

(viii) Needless to say that the results still depend on the input SSPs and especially on the *Response Functions* in use. This is a point of uncertainty that cannot be easily improved unless one has independent assessments of the quality of stellar models and calibrations. The *Response Functions*, in particular, are the major drawback of the whole problem because they are so far available only for three stars in total. A great deal of the results for the α -enhanced mixtures are still affected by the poor and coarse calibration at disposal. Tantaló et al. (2004) are currently working on this problem to provide *Response Functions* for a large grid of effective temperatures and gravities over the whole HR-Diagram, a large range of metallicities, and both solar and α -enhanced ratios. Some preliminary results of this study have already been anticipated in Sect. 5.2.

(ix) The sensitivity of indices like H_{β} to some abundance ratios (e.g. $[\text{Ti}/\text{Fe}]$ and likely other elements) adds another dimension to the interpretation of the two indices plane. We have indeed shown how in presence of enhancement ($\Gamma > 0$ and suitable ratios $[\text{X}_{\text{el}}/\text{Fe}] > 0$, $[\text{Ti}/\text{Fe}]$ in our case) an old galaxy could lie in the same region of a young one with solar abundance ratios. Were this the case, the observational spread in H_{β} could be the signature of different histories of star formation and chemical enrichment in turn passing from one galaxy to another. This topic has been carefully investigated in the companion paper by Tantaló & Chiosi (2004b) in which the suggestion is advanced that part of the scatter along the H_{β} axis observed in the H_{β} vs. $[\text{Mg}/\text{Fe}]$ plane could be attributed instead of the age, the current explanation, to a spread both in the degree of enhancement and some abundance ratios.

(x) There is an important remark to be made about the use of SSPs to simulate the complexity of a real galaxy. We have already touched upon this topic in Sect. 7.2, but it should be stressed once more here. In real galaxies, even in the case of EGs, a mix of stellar populations with different ages and chemical properties is likely to exist. Therefore the approximation to SSPs is no longer valid and SSPs should be replaced by galactic models incorporating the history of star formation and chemical enrichment and the indices to be used should take into account the contribution from all stellar components. Some of the properties shown SSPs, especially those caused by non standard evolutionary stages

(e.g. reversal of indices like H_{β} at increasing age and metallicity), that now have the same weight in the total balance of the resolving technique, are likely to smear out in the complex mix of stars because the contribution by each SSPs is proportional to the number of stars in the different age and metallicity bins. Integrated indices for model galaxies have been calculated by Tantaló et al. (1998) but never applied to this kind of analysis. This is a point that should be carefully investigated.

(xi) According to the results of this analysis and of previous ones as well, the conclusion one would draw is that EGs span very large ranges of age (and also of metallicity and enhancement in α -elements). The age is, however, the most embarrassing result. Does it mean that in galaxies, for which formal ages younger than the typical age of Globular Clusters (say 12 Gyr) are found, the bulk of stars have been formed at such young ages or there are effects to be taken into account? The question has been addressed for the first time by Bressan et al. (1996), explored in more detail by Longhetti et al. (2000), and also discussed by TFWG00. The question is: how much a recent, minute episode of star formation, engaging a small fraction of the total mass, may alter the indices of an otherwise old population of stars in EGs? The analyses was made by superposing to the indices of an old population of stars the variation caused by a recent episode of star formation. The result is that indices like H_{β} are strongly affected by even small percentages of young stars: as long as star formation is active they jump to very high values and when star formation is over they fall back to the original value on a time scale of about 1 Gyr. Other indices like Mg_2 , $\langle \text{Fe} \rangle$ are much less affected even if the companion chemical enrichment may somewhat change them. In diagnostics planes like H_{β} vs. $\langle \text{Fe} \rangle$ the galaxy performs an extended loop elongated towards the H_{β} axis, thus causing an artificial dispersion which could be interpreted as an age dispersions, whereas what we really see is the transient phase associated to the temporary stellar activity. The implications of this have carefully been investigated by Tantaló & Chiosi (2004b) with the aid of simulations of later star forming episodes of different intensity and age superposed to an old population of stars.

ACKNOWLEDGEMENTS

We would like to thank Roberto Caimmi, Laura Greggio, Ezio Pignatelli and Lorenzo Piovan for many stimulating discussions. We also thank Alberto Buzzoni for his very constructive comments as referee of the paper. This study has been financed by the Italian Ministry of Education, University, and Research (MIUR), and the University of Padua under the special contract "Formation and evolution of elliptical galaxies: the age problem".

REFERENCES

- Barbuy B., 1994, ApJ, 430, 218
- Bertelli G., Bressan A., Chiosi C., Fagotto F., Nasi E., 1994, A&AS, 106, 275
- Borges C. A., Idiart T. P., de Freitas-Pacheco J. A., Thevein F., 1995, AJ, 110, 2408

- Bressan A., Chiosi C., Fagotto F., 1994, *ApJS*, 94, 63
- Bressan A., Chiosi C., Tantalo R., 1996, *A&A*, 311, 425
- Brocato E., Matteucci F., Mazzitelli I., Tornambé A., 1990, *ApJ*, 349, 458
- Burstein D., Bertola F., Buson L. M., Faber S. M., Lauer T. R., 1988, *ApJ*, 328, 440
- Burstein D., Faber S. M., Gaskell C. M., Krumm N., 1984, *ApJ*, 287, 586
- Carney B., 1996, *PASP*, 108, 900
- Castellani V., Tornambé A., 1991, *apj*, 381, 393
- Chiosi C., Bertelli G., Bressan A., 1992, *ARA&A*, 30, 235
- Chiosi C., Carraro G., 2002, *MNRAS*, 335, 335
- Davies R. L., Kuntschner H., Emsellem E., Bacon R., Bureau M., Carollo C. M., Copin Y., Miller B. W., Monnet G., Peletier R. F., Verolme E. K., de Zeeuw P. T., 2001, *ApJL*, 548, L33
- Dorman B., Rood R. T., O'Connell R. W., 1993, *A&A*, 419, 516
- Faber S. M., Friel E. D., Burstein D., Gaskell C. M., 1985, *ApJS*, 57, 711
- Faber S. M., Worthey G., González J. J., 1992, in Barbuy B., Renzini A., eds, *The Stellar Population of Galaxies* IAU Symp. 149. Kluwer Academic Publishers: Dordrecht, p. 255
- Fagotto F., Bressan A., Bertelli G., Chiosi C., 1994, *A&AS*, 105, 39
- Girardi L., Bertelli G., 1998, *MNRAS*, 300, 533
- Girardi L., Bressan A., Bertelli G., Chiosi C., 2000, *A&AS*, 141, 371
- Girardi L., Bressan A., Chiosi C., Bertelli G., Nasi E., 1996, *A&A*, 117, 113
- González J. J., 1993, PhD thesis, University of California, Santa Cruz
- Gratton R., Carretta E., Claudi R., Lucatello S., Barbieri M., 2003, *A&A*, 404, 187
- Green E., Demarque P., King C., 1987, *The revised Yale isochrones and luminosity functions*. New Haven: Yale Observatory, 1987
- Greggio L., Renzini A., 1983, *A&A*, 118, 217
- Greggio L., Renzini A., 1990, *ApJ*, 364, 599
- Grevesse N., Noels A., Sauval A., 1996, in Holt S., Sonneborn G., eds, *Cosmic Abundances* ASP Conf. Ser. 99. San Francisco: ASP, p. 117
- Habgood M.-J., 2001, PhD thesis, Univ. of North Carolina at Chapel Hill
- Horch E., Demarque P., Pinsonneault M., 1992, *ApJ*, 388, L53
- Idiart T. P., de Freitas-Pacheco J. A., 1995, *AJ*, 109, 2218
- Jørgensen I., 1999, *MNRAS*, 306, 607
- Kuntschner H., 1998, PhD thesis, Univ. of Durham
- Kuntschner H., 2000, *MNRAS*, 315, 184
- Kuntschner H., Davies R. L., 1998, *MNRAS*, 295, L29
- Kuntschner H., Lucey J. R., Smith R. J., Hudson M. J., Davies R. L., 2001, *MNRAS*, 323, 615
- Larson R. B., 1974, *MNRAS*, 142, 501
- Leitherer C., Alloin D., v. Alvensleben U. F., Gallagher J., Huchra J., et al. 1996, *PASP*, 108, 996
- Longhetti M., Bressan A., Chiosi C., Rampazzo R., 2000, *A&A*, 353, 917
- Maraston C., 1998, *MNRAS*, 300, 872
- Maraston C., Greggio L., Renzini A., S.Ortolani Saglia R., Puzia T., Kissler-Patig M., 2003, *A&A*, 400, 823
- Marigo P., Chiosi C., Kudritzki R.-P., 2002, *A&A*, p. 617
- Matteucci F., 1994, *A&A*, 154, 279
- Matteucci F., 1997, *Fundam. Cosmic Phys.*, 17, 283
- Matteucci F., Ponzzone R., Gibson B. K., 1998, *A&A*, 335, 855
- Munari U., Sordo R., Castelli F., Zwitter T., 2004, *A&A*, to be submitted
- Pagel B. E. J., 1989, in Beckman J., Page B. E. J., eds, *Evolutionary Phenomena in Galaxies* Cambridge University Press: Cambridge, p. 201
- Peimbert A., Peimbert M., 2002, in *Revista Mexicana de Astronomia y Astrofisica Conference Series A New Determination of the Primordial Helium Abundance*. pp 250–250
- Poggianti B., Bridges T., Mobasher B., Carter D., Doi M., Iye M., Kashikawa N., Komiyama Y., Okamura S., Sekiguchi M., Shimasaku K., Yagi M., Yasuda N., 2001, *ApJ*, 562, 689
- Reimers D., 1975, *Mem. Soc. R. Sci. Liege*, ser. 6, 8, 369
- Renzini A., Buzzoni A., 1986, in Chiosi C., Renzini A., eds, *Spectral Evolution of Galaxies* Dordrecht: Riedel, p. 213
- Ryan S., Norris J., Bessell M., 1991, *AJ*, 102, 303
- Salasnich B., Girardi L., Weiss A., Chiosi C., 2000, *A&A*, 361, 1023, (SGWC00)
- Salvaterra R., Ferrara A., 2003, *MNRAS*, 340, L17
- Tantalo R., 1998, PhD thesis, Univ. of Padova
- Tantalo R., Chiosi C., 2004a, *MNRAS*, in preparation
- Tantalo R., Chiosi C., 2004b, *MNRAS*, accepted
- Tantalo R., Chiosi C., Bressan A., 1998, *A&A*, 333, 419
- Tantalo R., Chiosi C., Bressan A., Marigo P., Portinari L., 1998, *A&A*, 335, 823
- Tantalo R., Chiosi C., Munari U., Piovani L., Sordo R., 2004, *MNRAS*, submitted
- Thomas D., Maraston C., 2003, *A&A*, 401, 429
- Thomas D., Maraston C., Bender R., 2003a, *MNRAS*, 339, 897, (TMB03)
- Thomas D., Maraston C., Bender R., 2003b, *MNRAS*, 343, 279
- Trager S., 1997, PhD thesis, Univ. of California, Santa Cruz
- Trager S. C., Faber S. M., Worthey G., González J. J., 2000a, *AJ*, 120, 165
- Trager S. C., Faber S. M., Worthey G., González J. J., 2000b, *AJ*, 119, 1645, (TFWG00)
- Tripicco M. J., Bell R. A., 1995, *AJ*, 110, 3035, (TB95)
- Vandenberg D., 1985, *ApJS*, 58, 711
- Vandenberg D., Bell R., 1985, *ApJS*, 58, 561
- Vandenberg D., Laskarides P., 1987, *ApJS*, 64, 103
- Vassiliadis D. A., Wood P. R., 1993, *ApJ*, 413, 641
- Vazdekis A., Kuntschner H., Davies R. L., Arimoto N., Nakamura O., Peletier R. F., 2001, *apj*, 551, 127
- Weiss A., Peletier R. F., Matteucci F., 1995, *A&A*, 296, 73
- Worthey G., 1992, PhD thesis, Univ. of California
- Worthey G., 1994, *ApJS*, 95, 107
- Worthey G., Faber S. M., González J. J., 1992, *ApJ*, 398, 69
- Worthey G., Faber S. M., González J. J., Burstein D., 1994, *ApJS*, 94, 687
- Worthey G., Ottaviani D., 1997, *ApJS*, 111, 377